https://ntrs.nasa.gov/search.jsp?R=19660010669 2020-03-16T22:41:21+00:00Z

TYCO LABORATORIES, INC., BEAR HILL, WALTHAM, MASSACHUSETTS 02154 TELEPHONE 617 899-1650

FACILITY FORM 602

N66-19958 (ACCESSION NUMBER) (THRU)
58 (PAGES) 1 (CODE)
CR 70710 (NASA CR OR TMX OR AD NUMBER) 15 (CATEGORY)

GPO PRICE $
CFSTI PRICE(S) $
Hard copy (HC) 3.00
Microfiche (MF) .50
ff 653 July 65

LEAD TELLURIDE NON-MAGNETIC BONDING RESEARCH STUDY

Second Quarterly Report
for period June 1 through
August 31, 1965

Contract Number NAS5 -9149

Prepared for

National Aeronautics and Space Administration
Goddard Space Flight Center
Greenbelt, Maryland

Tyco Laboratories, Inc.
Bear Hill
Waltham, Massachusetts 02154

LEAD TELLURIDE NON-MAGNETIC BONDING RESEARCH STUDY

Second Quarterly Report
for period June 1 through August 31, 1965

by
H. E. Bates
M. Weinstein

NASA CR 70710

Contract Number NAS 5-9149

Prepared for

National Aeronautics and Space Administration
Goddard Space Flight Center
Greenbelt, Maryland

Contents

ABSTRACT

19958

The purpose of this study is to define in fundamental terms the most appropriate system and process for the reproducible fabrication of low-resistance, high-strength bonds of non-magnetic electrodes to PbTe and PbTe-SnTe thermoelectric alloys. During this period SnTe braze-bonding of Ta and W electrodes to $Pb_{.5}Sn_{.5}Te$ thermoelements was studied, in addition to investigating diffusion bonding of W electrodes to $Pb_{.5}Sn_{.5}Te$. Some diffusion-bonded elements were examined by the electron beam microprobe technique. The designing of a sixteen-specimen, gradient life testing device was completed. Physical and chemical evaluation of commercially available thermoelements was continued.

Author

I. INTRODUCTION

This program comprises an investigation of the bonding of PbTe and PbTe-SnTe thermoelements to non-magnetic electrodes, and a study of the physical and chemical factors contributing to the degradation and failure of such thermocouples during extended operation. The bonding studies are directed toward the optimization of procedures for diffusion- and braze-bonding of W and Ta electrodes to n- and p-type PbTe and PbTe-SnTe. The studies of degradation and failure are aimed at elucidating the processes involved in the long-term deterioration of thermoelement properties. By obtaining some idea of the kinetics of these processes, it should be possible to predict the long-term behavior of bonded thermoelements.

Work during this quarter has been concerned with bonding of Ta and W electrodes to p-type PbTe-SnTe thermoelements by brazing and diffusion; fabrication and measurements of segmented SiGe-PbTe couples using diffusion bonding; design of a multi-element life testing fixture; and continued evaluation of the physical and chemical factors inherent in the structure of available thermoelements which may affect their behavior.

II. BONDING STUDIES

A. P-type PbTe-SnTe Diffusion Bonding

Attempts to bond p-type elements by diffusion to W electrodes were almost completely unsuccessful, as noted in the First Quarterly Report. Variation of all the major variables of the bonding process produced no improvement. Outgassing of the elements with resultant oxidation of the electrode was highly suspect as the cause of the difficulties. Electrodes and bonding weights, both of tungsten, often showed very obvious oxide films. The bonding jig was redesigned to test this possibility. The circumferential clearance had been reduced in the n-type jigs to .005 to .010" to provide better alignment of the electrode-element-weight assembly. The same clearances were provided in the new p-type jigs. When the holes were bored out to give about .035" clearance, p-type elements from batches which had consistently failed to bond started to yield low resistance bonds.

Thus, one solution to the problem of the high oxygen content of the p-type material appears to be to provide free access for the flowing gas stream to the element. Ideally, the element should be completely exposed to provide maximum outgassing; in practice this is not possible. However maximum "ventilation" should be provided in any bonding apparatus used for this material.

Vacuum fusion analyses have shown the average (of six samples) oxygen content of new p-type elements to be 435 ppm. The average oxygen content of two elements which had been successfully diffusion-bonded and then broken from their electrodes was 320 ppm. This represents a 25% reduction in the total oxygen content of the elements. Three hundred ppm oxygen is still a far from satisfactory level and degassing during the actual bonding process is also not desirable. The major barrier to any effective degassing process, either vacuum or flowing inert gas, is the high evaporation rate of PbTe and PbTe-SnTe at temperatures over 500°C, which temperatures are, of course, necessary to complete the degassing in a reasonable length of time.

Preparation of elements and electrodes for all diffusion bonding experiments was essentially the same as previously employed. In one case the elements were mounted on the parallel block and the interstices filled with mounting wax before lapping. This was done to prevent chipping of the corners of the elements. Electrodes were lapped to 1800 grit generally, in some cases to 180 grit. Bonding was accomplished at 830 - 840°C for 15 - 20 minutes with a single pressure of 30 g/cm^2. The elements and electrodes as removed from the bonding fixture were bright and clean.

Results of some measurements on diffusion-bonded elements are shown in Fig. 1. The difference between the curves for new, unbonded elements and diffusion bonded elements should not be regarded as at all serious. Ten new elements were measured under the same conditions as the bonded elements, i.e. 5/32" W electrodes were placed on either end to approximate the same thermal conditions as are seen by the bonded elements. The results of these measurements were exactly the same as those for the bonded elements. This indicates that the bonded elements are

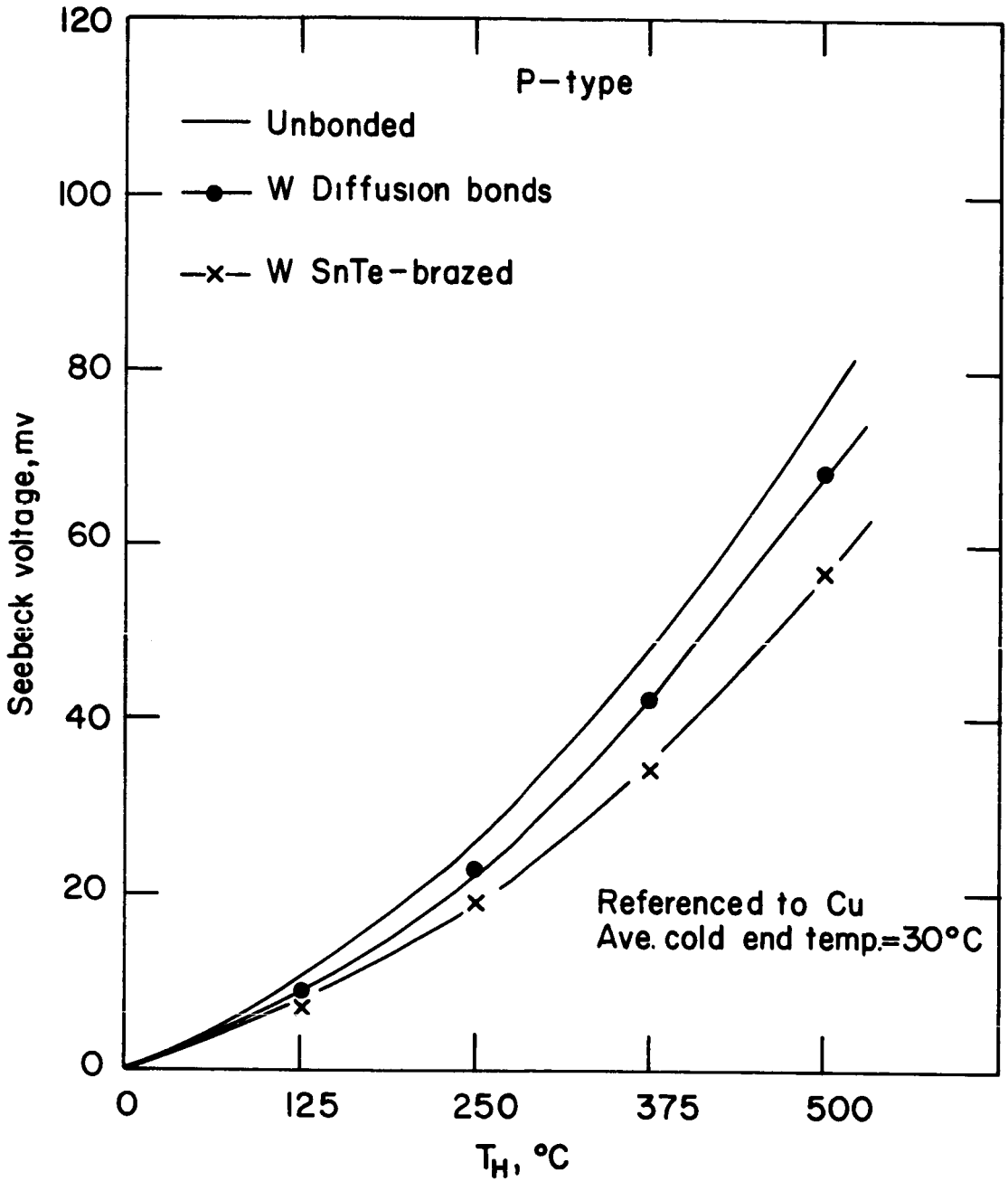

Fig. 1 Seebeck voltage output as a function of temperature for $Pb_{.5}Sn_{.5}Te$ elements bonded to W electrodes by diffusion and SnTe brazing.

only slightly degraded in output, if at all, by the bonding process. The lower thermal resistance of the diffusion bond should provide a somewhat greater temperature difference over the length of the element than that which would be found in the loose assembly; thus, if the bonded element has the same total output, its average Seebeck coefficient is probably slightly lower than that of a new element, since

$$S = \int_{T_1}^{T_2} \alpha(T)\, dT \quad \text{or} \quad S \cong \bar{\alpha}\, \Delta T .$$

Measurements of the contact resistance on eighteen bonded elements show an over-all average bond resistance of 89 $\mu\Omega$ at room temperature. Some 70% of these contacts had resistances less than 100 $\mu\Omega$ (it is felt that this represents the upper limit of acceptable bond resistance), and the average resistance of this group was 60 $\mu\Omega$, equivalent to 20 $\mu\Omega\text{-cm}^2$. Only one bond (out of 36) failed to diffuse, and the highest resistance encountered was less than 200 $\mu\Omega$. Bond strengths seem to be quite high; it was necessary to use pliers to remove the electrodes from two elements used in gas analysis. Measurements of the variation of resistance with temperature have not yet been made; however, the small change in Seebeck voltage indicates a correspondingly small change in resistivity behavior.

These results are very encouraging, since no systematic effort has been made to improve the bonding process for p-type diffusion bonding and we do know from isolated examples made under the previous contract (NAS 5-3986) that very low bond resistances (20 $\mu\Omega$ or less) can be achieved by diffusion bonding of p-type PbTe-SnTe to W. Considerably more study is necessary for this system, in particular investigation of bond stability. The high oxygen content of the p-type elements represents a serious threat to the integrity of the bond at temperature.

B. P-type PbTe-SnTe Braze-bonding

Bonding of p-type elements to Ta and W electrodes by SnTe brazing was re-examined. Brazing of W with SnTe had not been investigated during the initial contract, and thus was studied here for the first time. The com-

bination Ta-SnTe , on the basis of rather limited evidence, was chosen initially as a satisfactory method of bonding to PbTe-SnTe (and to PbTe). Results of this recent investigation indicate that the use of SnTe can cause considerable difficulty in the brazing of PbTe-SnTe.

1. W-SnTe Brazing

Some experience had been gained with the SnTe-W combination during the previous quarter. Initial indications were that a means of removing the oxide from the W surface was necessary to ensure good wetting by the SnTe. More recently, it has been found that by using a large amount of braze (to compensate for evaporation losses) and holding at 840° - 850° for 20 - 30 minutes, excellent wetting can be achieved. The braze layer can be ground to any desired thickness with relative ease. Various braze thicknesses were used from 15 mils to 3 mils. The thicker braze layers tended to spill excess braze (plus a certain amount of material from the element dissolved in the braze) onto the side of the element. When the excess braze was removed, a system of cracks could be seen on the element surface. This cracking was attributed to the spilled braze at first; however, when thin braze layers were used, the cracks still developed (see Fig. 2).

Resistance measurements confirmed the presence of the cracks in the bulk of the elements. Where the bond was intact, contact resistance was very low, less than 5 $\mu\Omega$; however, generally, cracks existed in the bond region or fairly near it. Figure 3 shows cracks in the element propagating from the bond region of a W SnTe-brazed element. When the electrodes were broken from the elements, a rim of material was usually left on the electrode so that the end of the broken element was in the shape of a truncated cone. That this fracture pattern was the result of the pre-existing cracks is obvious from Figs. 2 and 3. The Seebeck voltage output of SnTe-brazed W bonded elements is shown in Fig. 1. Allowing for the effect of the thick electrodes (roughly the difference between the unbonded and the diffusion bonded curves), it is still apparent that the W SnTe-brazing process has caused a 15 - 20 percent decrease in output. Resistances were generally double or treble those of an unbonded element due to the cracking. Room temperature resistivity was not changed appreciably.

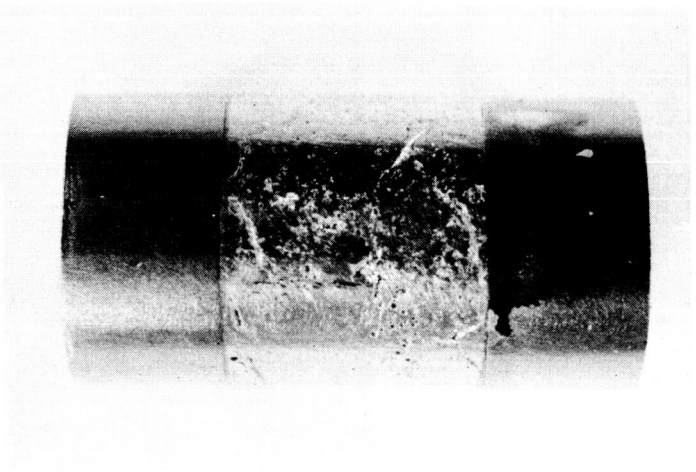

Fig. 2 P-type element SnTe-brazed to W electrodes showing surface cracks X7.

Fig. 3 Microsection of SnTe-brazed W electrode on p-type showing extensive internal cracking X70.

2. Ta-SnTe Brazing

The combination of Ta electrode and SnTe braze was found rather early in the program to provide excellent wetting and an extremely strong bond. With n-type PbTe the SnTe-Ta combination provided low resistance, high strength bonds, the only stricture being the necessity to dope the SnTe n-type. The few p-type samples brazed to Ta with SnTe also showed excellent properties. Studies to evaluate the Ta-SnTe combination with $Pb_{.5}Sn_{.5}Te$ p-type elements more thoroughly have shown that considerable difficulties may be experienced in its use.

Tantalum electrodes 0.150" thick by 0.250" in diameter were prewetted with SnTe by heating to 820°C for 10 min. The SnTe was then ground to the desired thickness. Brazing of the electrodes to the elements was accomplished by heating to slightly over the melting point of SnTe (805°C) for about five minutes. Cooling rates of approximately 6°C/min and 12-15°/min were used. The photograph of the W bonded element in Fig. 2 typifies the results obtained with Ta. Figures 4 and 5 show two sections of the same element about 50 mils apart on a radius. The orientation of the element is the same in both pictures. At the left-hand end of Fig. 5 a crack can be seen running parallel to the bond at the center of the element. After varying braze thickness and cooling rates with the thick electrodes, 10 mil Ta sheet electrodes were tried. It was thought that the "stiffness" of the thick electrodes might be the cause of the cracking; and it was observed when brazing and bonding n-type with Ta sheet that often the electrode took on a dished shape due to the greater contraction of the braze. However, results with the thin electrodes on p-type showed no improvement. Figure 6 shows sections of two Ta-SnTe-brazed elements with extensive cracking in the bulk of the element. Close inspection of the macrophotos (Figs. 4 - 6) reveals a band of uniform thickness and contrasting appearance at the interface of electrode and element. Examination of a polished section of a Ta-bonded element showed that this band was, in fact, made up of what can be assumed to be the braze layer filled with randomly precipitated crystals of a second phase as shown in Fig. 7. Figure 7b shows the same structure at a higher magnification. The other features of Fig. 7 to note are the row of pores a short distance from the area of precipated crystals

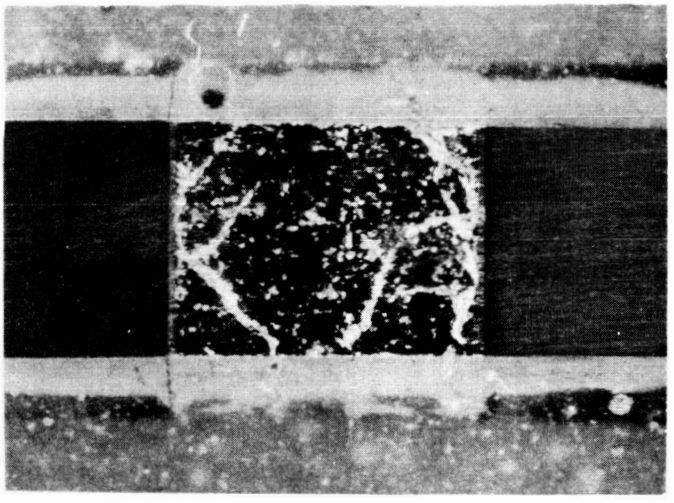

Fig. 4 Section of SnTe-brazed Ta bonded p-type element showing pattern of internal cracks X7.

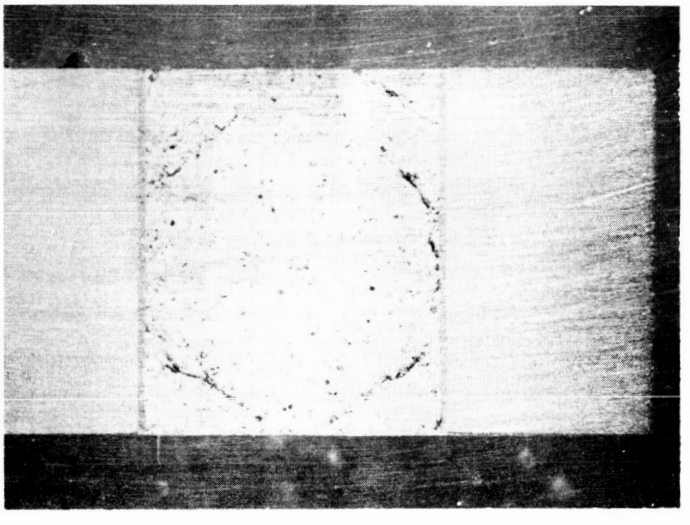

Fig. 5 Same element as Fig. 4; section is .050" closer to center of element X7.

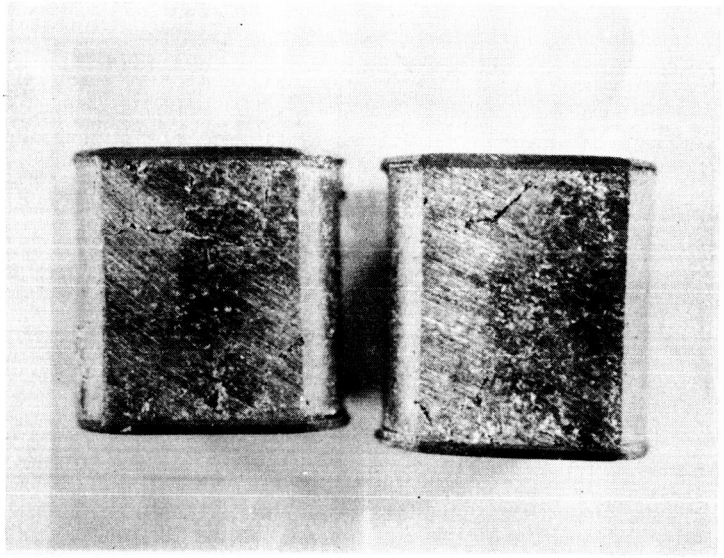

Fig. 6 Ten mil Ta electrodes SnTe-brazed on p-type elements. Extensive internal cracking is evident X7.

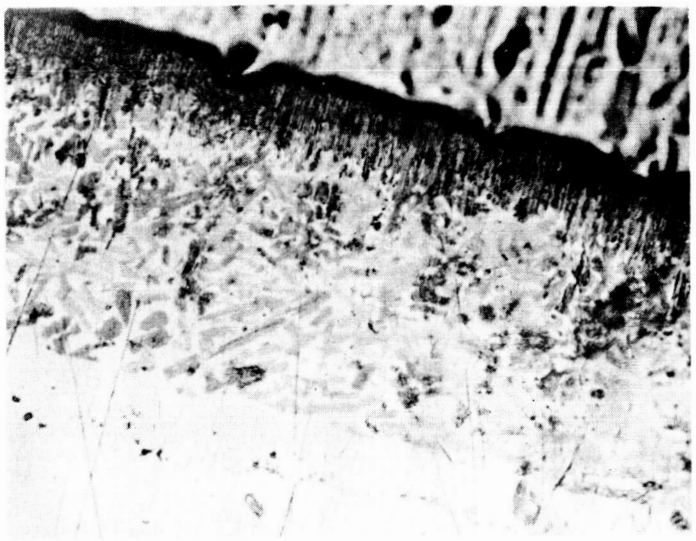

Fig. 7a Second phase precipitation in SnTe braze layer on Ta electrode X500.

Fig. 7b Same as 7a X1000.

and parallel to it - these mark the original interface between the braze and the element as indicated by the thickness of the braze layer before bonding - and the layer of apparently columnar crystals along the interface of braze and electrode. This columnar layer is not so obviously present in sections of as-brazed electrodes; nor, in fact, does there seem to be as great a concentration of the second phase as in the bonded specimens (e.g. Fig. 7), although the width of the area of precipitation is about equal in both cases. Despite the lack of any other confirming evidence at this time, it seems reasonable to assume that the precipitated crystals in Fig. 7 are either $TaTe_3$ and/or $TaTe_2$. The existence and structures of $TaTe_3$ and $TaTe_2$ have been reported by Ukrainskii, et al [1], and Brixner [2].

The presence of a reaction zone of tantalum tellurides is not a priori harmful. Brixner [2] gives a room temperature resistivity for $TaTe_2$ of the same magnitude as the $Pb_{.5}Sn_{.5}Te$, while the Seebeck coefficient is low and n-type. This is confirmed by our measurement of very low contact resistances where the bond has remained intact. However, instances of cracks running from, or into, the columnar layer of the reaction zone were observed. Whether the telluride formation caused the cracks is open to question. In the case of W electrodes, where no telluride formation was observed, cracking also occurred. Therefore, there seems to be reason to believe that the tantalum tellurides do not contribute as a first cause to the cracking of the bond and element.

The Seebeck voltage output curves for SnTe-brazed Ta-bonded elements are given in Fig. 8. If allowance is made for the lowering in output due to the thick electrodes, it can be seen that the 0.150" electrode samples suffer fairly little degradation. However, the 10 mil electrodes, which should cause much less loss from thermal resistance, show a reduction in output of at least 10 percent. Total element resistances were generally at least double that of an unbonded element due to internal cracking, while bond resistances (uncracked) were very low and bulk resistivity was virtually unchanged.

The problem of cracking of brazed p-type elements seems to be associated with the combination of braze and electrode. The presence of braze alone has been shown not to cause cracking in the element. (An

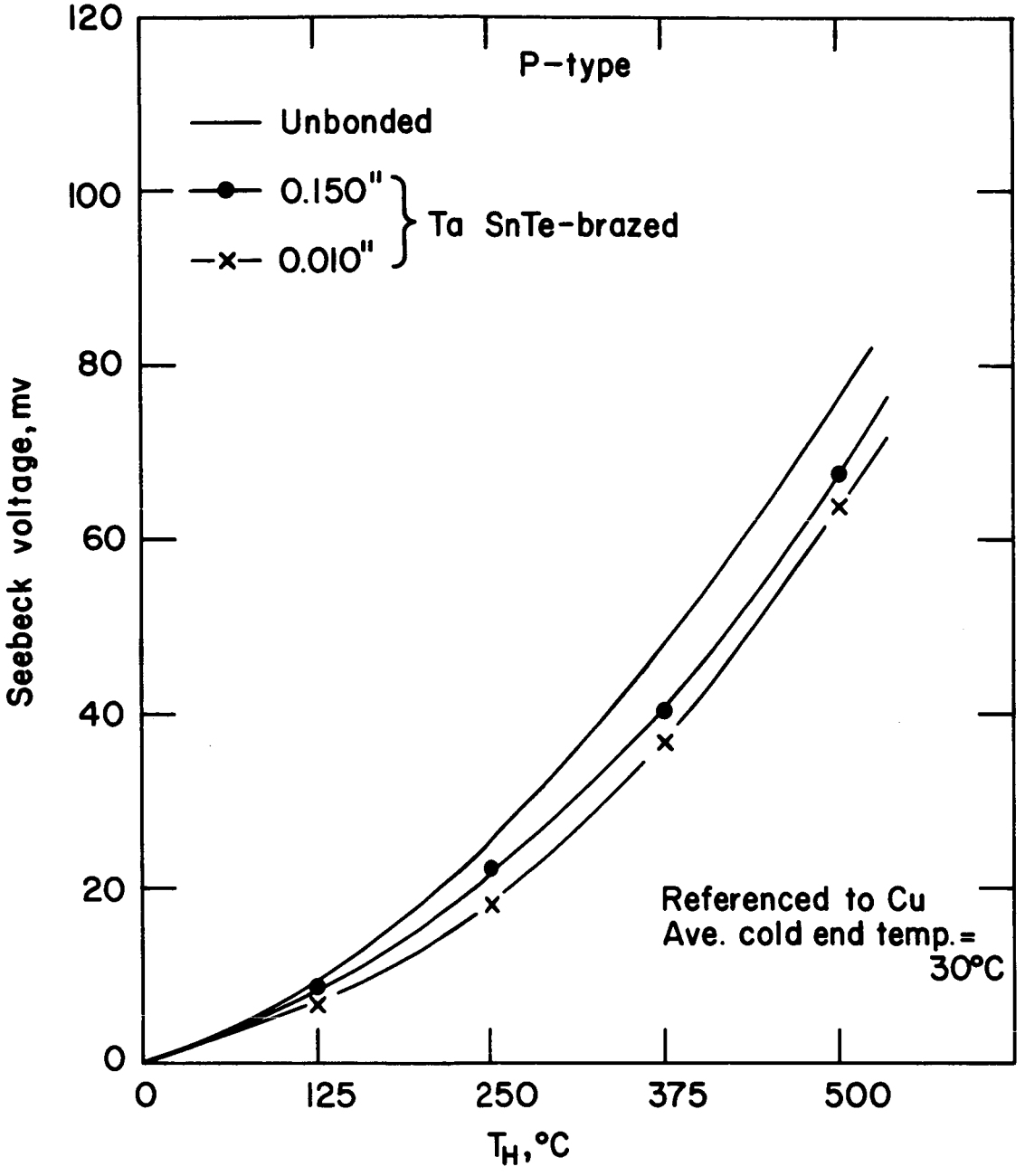

Fig. 8 Seebeck output voltage as a function of temperature for SnTe-brazed Ta electrodes of two thicknesses bonded to $Pb_{.5}Sn_{.5}Te$ elements.

experiment was done in which SnTe was melted onto the free upper surface of p-type elements with the same time-temperature cycle as that used in the braze-bonding procedure.) The absence of cracking in diffusion-bonded elements serves to indicate that, at least for W , the electrode by itself (in a sense) is not at fault. The presence of a second phase at the interface is also not directly responsible, since no telluride formation can be found in the brazed W specimens. The important feature of any analysis of this situation is that the presence of a braze layer increases the transfer into the element of the stresses due to mismatch of expansion coefficients between element and electrode.

Hittman Associates [3] presented an analysis of the stresses in a brazed element with an electrode of different expansion coefficients, and presented experimental evidence to indicate that p-type PbTe with Fe electrodes fractured due to thermal stresses. The mismatch of expansion coefficients of Ta and $Pb_{.5}Sn_{.5}Te$ is even greater than that of Fe and PbTe, so it is not surprising to encounter cracking in this system. Consideration of the stress pattern in this system leads us to the same general state of stress as that shown by Hittman. That is, an annulus of shear stress exists within the periphery of the bond region of sufficient magnitude to fracture the thermoelectric element. Hittman Associates feels, however, that the cracks grow parallel to the axis of the element and should not markedly affect the conductivity of the element or cause separation of the joint. We have seen that the cracks in Ta-bonded elements grow at a distinct angle to the axis of the element, and that often a crack covers the central portion of the element not in, but very near the bond and parallel to it. This indicates (1) that the shear stress does not tend to zero at the center of the element and (2) that the longitudinal (axis) stress is sufficient to force cracks started at the bond to grow outwards (due to the variation from compressive stress at the center line to tensile at the surface of the element) to the surface of the element (see Fig. 5).

Our experience with Ta braze-bonding to n-type PbTe has been that the strength of $Pb_{.5}Sn_{.5}Te$ p-type material would be sufficient to resist the stresses encountered in bonding to Fe electrodes. It appears, however, from the very poor results thus far with Ta braze-bonding to $Pb_{.5}Sn_{.5}Te$,

that brazing to any of the low-expansion refractory metals may be virtually impossible.

C. Electron Beam Microprobe Studies

Tungsten diffusion-bonded PbTe and $Pb_{.5}Sn_{.5}Te$ elements were examined in the bond areas with an electron beam microprobe analyzer [5]. Difficulty was experienced with grooving at the interface in some samples due to polishing. The most successful method of preparing the surface was found to be careful grinding to 600 grit, rather than polishing. The interface is sharply defined by this method as can be seen in Fig. 9. A relatively scratch-free area is then selected for examination.

Results of a number of traverses on n- and p-type samples diffusion-bonded to W indicated a definite absence of compound formation or precipitation in the area of the bond. A shallow diffusion zone about two microns wide apparently exists as can be seen from Figs. 10 and 11, which are direct reproductions of the traces made in scanning the bond shown in Fig. 9. The first trace was made from electrode to element, analyzing for Te radiation. The direction of travel was then reversed to analyze for Pb radiation (Fig. 11). The line perpendicular to the bond on the left side of Fig. 9 is contamination from the beam and shows the exact path of the scan. The resolution of the analyzer in traversing a very narrow zone is limited by the diameter of the beam spot, about three microns. It is for this reason that the distance covered in going from 100% of one element to zero is about five microns on the chart. The elements examined were all as-bonded, i.e. with no thermal history, other than bonding. One n-type element was scanned which had been held at 600° for 500 hours. There was no appreciable broadening of the diffusion zone.

D. SiGe-PbTe Segmented Thermoelements

A number of thermoelements, both n- and p-type, were prepared by bonding 0.438" diameter PbTe and $Pb_{.5}Sn_{.5}Te$ elements to SiGe thermoelements. The lead telluride elements were diffusion-bonded to W shoes which had been fusion-bonded to the SiGe by the manufacturer (RCA). The bonding process was unchanged from that previously used in bonding

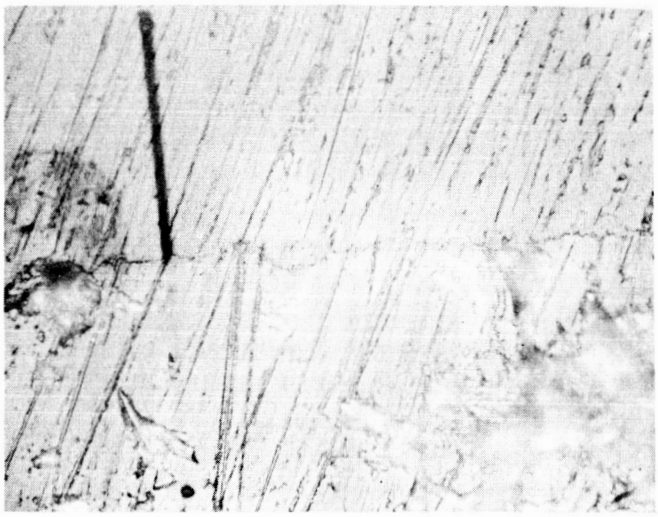

Fig. 9 N-type PbTe element with W diffusion-bonded electrode at top, 600 grit surface X500.

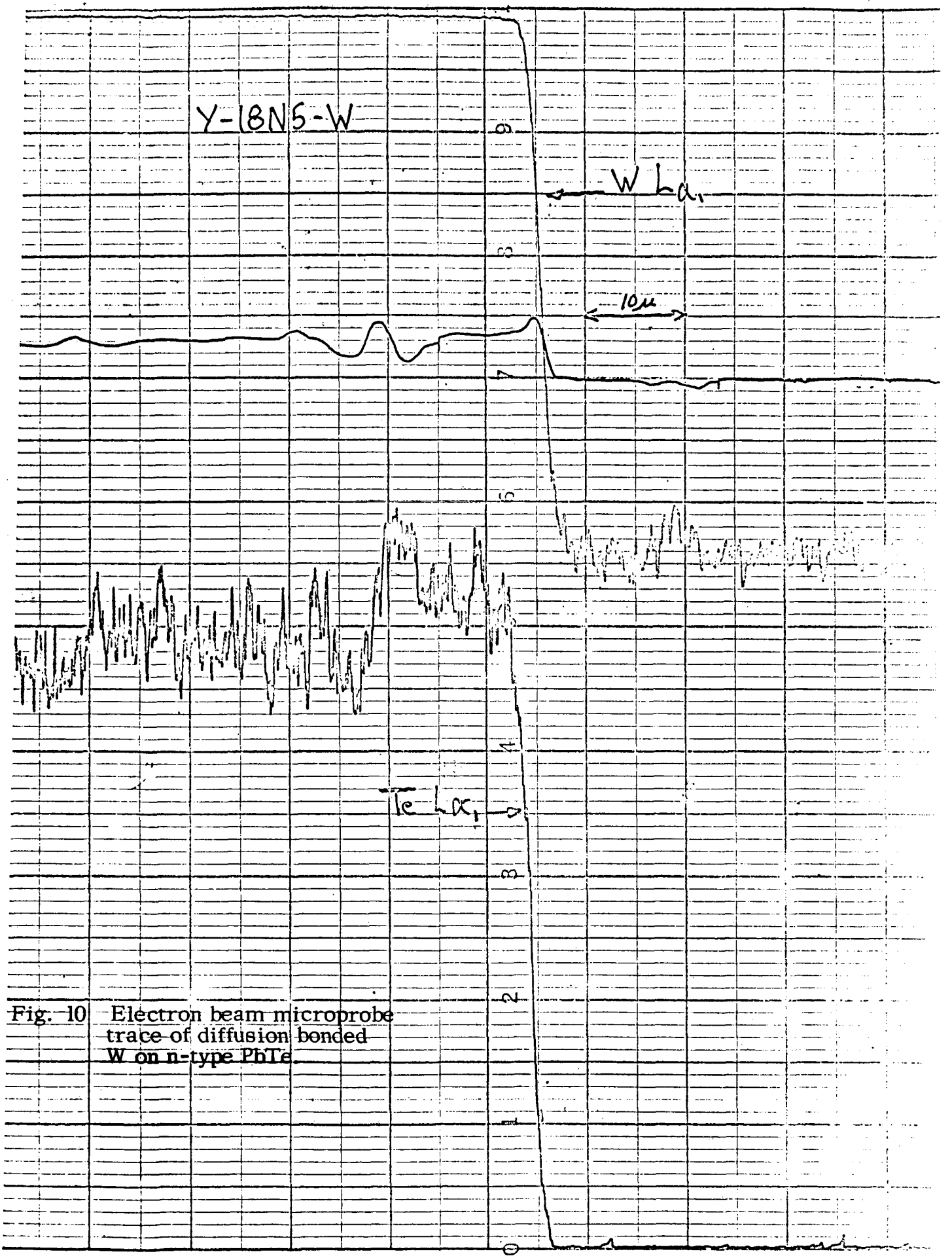

Fig. 10 Electron beam microprobe trace of diffusion bonded W on n-type PbTe.

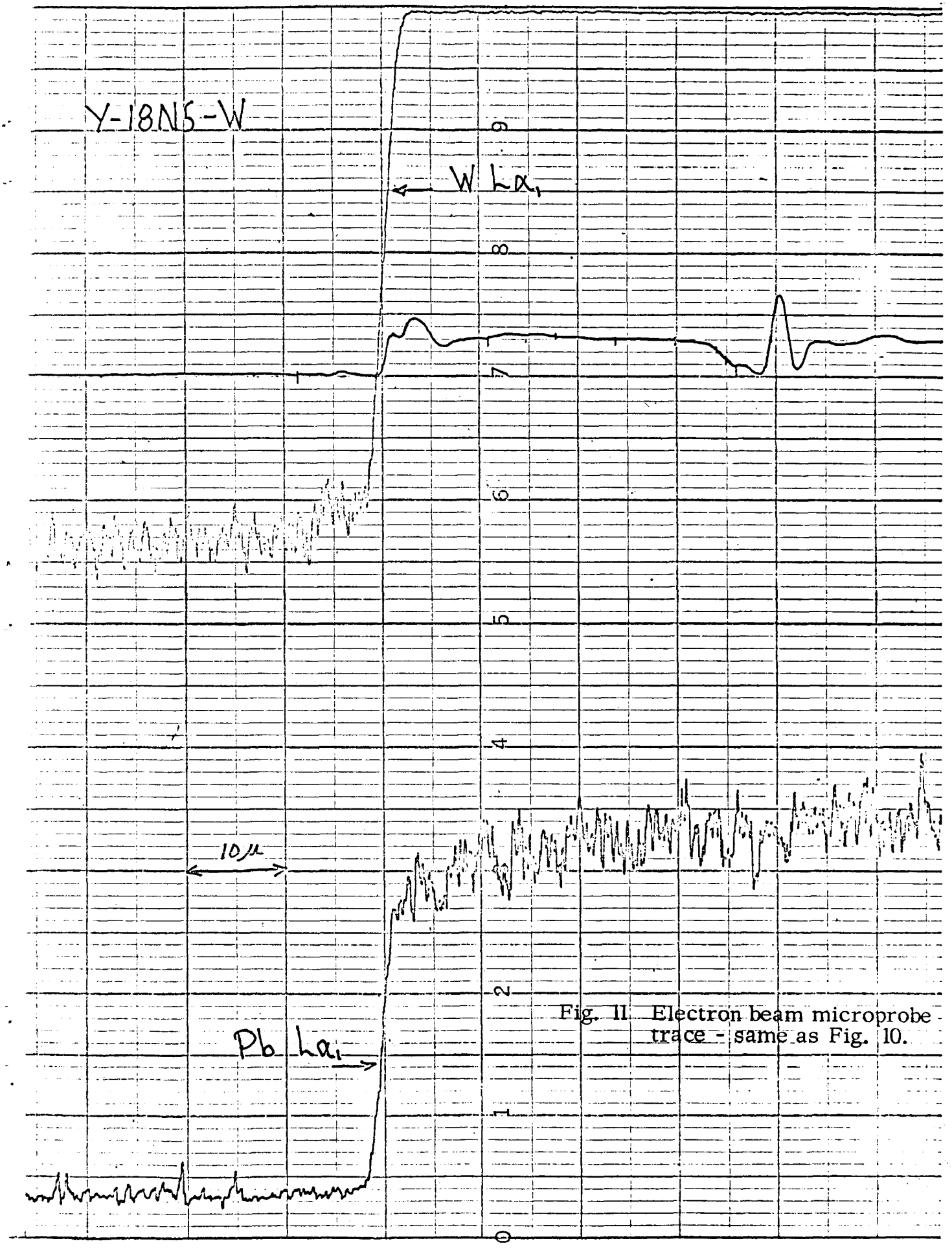

Fig. 11 Electron beam microprobe trace - same as Fig. 10.

to 0.250" W electrodes. Contact resistances at room temperature were characteristically 20 $\mu\Omega$ for n-type PbTe, while the lowest p-type resistances were about 35 $\mu\Omega$ with others in the 80 - 100 $\mu\Omega$ range. Tin telluride brazing of the $Pb_{.5}Sn_{.5}Te$ elements was tried initially with very little success. The bonds that resulted were high resistance and very weak mechanically.

Measurements of resistance and output voltage were made on a number of the segmented elements up to hot junction temperatures of 800°C. Pure nickel lead wires were soldered into slots on the cold end of the lead telluride section and spot-welded to the W hot shoe of the SiGe. A 3 mil chromel-alumel thermocouple was spot-welded to the central W shoe. Hot and cold end temperatures were measured with chromel-alumel thermocouples spring-loaded against the ends of the element.

The next two pages present, in condensed form, the average results obtained from these measurements.

Performance Data of Si-Ge - PbTe Segmented Elements

(1) N-type

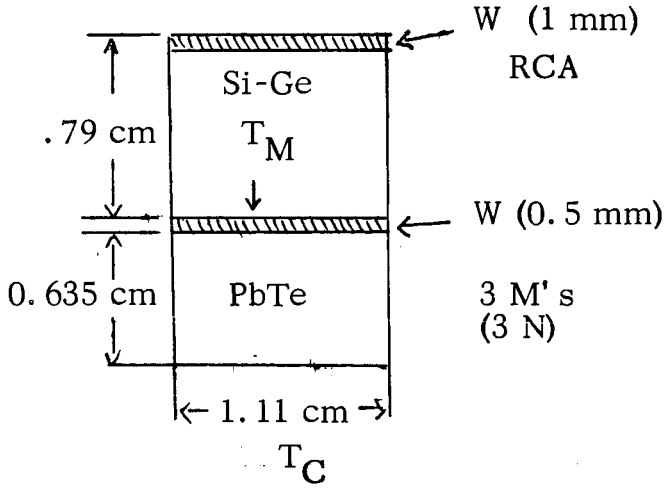

T_H = 800°C

T_M = 525°C

T_C = 115°C

Voltage Output = 145 mv
(referenced to Cu)

R_{Total} = 3.8 mΩ

$$\text{Power} = \frac{V^2}{4R} = \frac{(145)^2}{4 \times 3.8} = 1.38 \text{ w}$$

$$Q_{\substack{\text{Si-Ge} \\ 800\text{-}525^\circ\text{C}}} = KA\frac{\Delta T}{\Delta X} = \frac{0.037 \times 0.93 \times 275}{0.79} = 11.9 \text{ w}$$

$$Q_{\substack{\text{PbTe} \\ 525\text{-}115}} = \frac{0.018 \times 0.96 \times 410}{0.635} = 11.3 \text{ w}$$

$$Q_{Average} = 11.6 \text{ w}$$

$$\text{Efficiency} = \frac{\text{Power out}}{\text{Power in}} = \frac{1.38}{11.6} = 11.9\%$$

(2) P-type

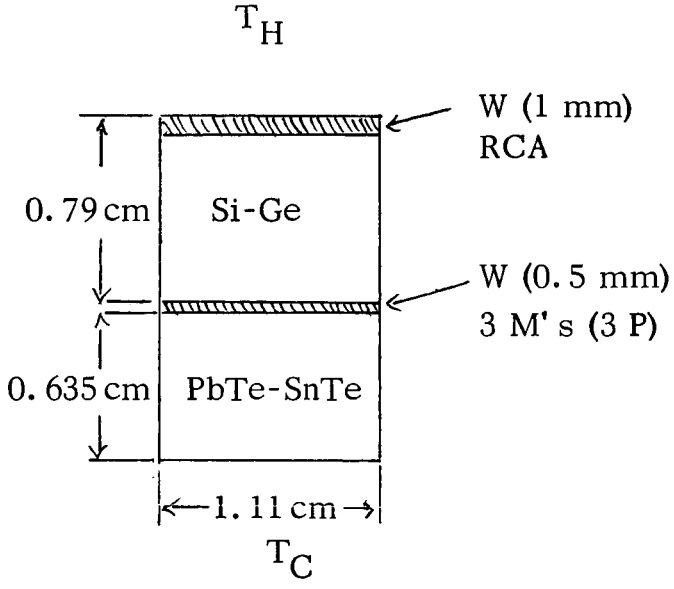

T_H = 800°C

T_M = 540°C

T_C = 145°C

Voltage Output = 142 mv
(referenced to Cu)

R_{Total} = 380 mΩ

$$\text{Power} = \frac{V^2}{4R} = \frac{(142)^2}{4 \times 3.8} = 1.32 \text{ w}$$

$$Q_{\substack{\text{Si-Ge} \\ 800\text{-}550}} = \frac{0.041 \times 0.93 \times 250}{0.79} = 12.1 \text{ w}$$

$$Q_{\substack{\text{PbTe} \\ 540\text{-}145°C}} = \frac{0.013 \times 0.96 \times 395}{0.46} = 10.7 \text{ w}$$

$Q_{Average}$ = 11.4 w

$$\text{EFF} = \frac{\text{Power Out}}{\text{Power In}} = \frac{1.32}{11.4} = 11.6\%$$

Total power output per couple 2.7 w with an average efficiency of 11.7%.

III. THERMOELECTRIC LIFE TEST STATION

A multi-element life test station for extended operation, under a gradient, of sixteen thermoelements has been designed. Initial design considerations called for efficient operation, maximum elements on test, and compatibility of the design with automatic data acquisition equipment to facilitate monitoring of thermoelectric properties during extended testing. The design, which is detailed in the appendix, consists of an electrically and thermally common resistance heater and individual, isolated water-cooled blocks which can support a gradient from 800°C to 25°C across sixteen thermoelements of 0.25" - 0.50" diameter by 0.25" - 1.00" length. Hot and cold junctions are provided with individual thermocouples. Thus, measurements are possible on hot junction temperature, cold junction temperature, open-circuit output voltage, and total element resistance. The mechanical assembly is supported in a bell jar enclosure with all the necessary feed-throughs for water, electrical power, and electrical measurements. Supporting equipment such as heater controller, measurement apparatus, gas and water valving and regulators, and vacuum pump will be consolidated in a test stand.

The life test station was designed and all components chosen to provide maximum reliability over extended periods of operation. Failure of one or more thermoelements or their thermocouples will not affect the testing of the others. A reasonable range of element sizes can be accommodated and a variety of sizes can be tested simultaneously. The cold junctions automatically adjust to any misalignment of the element due to nonparallel ends. The circular arrangement of the element stations provides equally easy access to all for convenience of loading and adjustment. Sufficient space around the mechanical assembly has been provided to facilitate servicing; this would not have been possible if a greater number of elements were to be tested. The electronic measurement instrument configuration is arranged so that properties may be measured manually or electronically.

IV. N-TYPE LIFE TESTING

Preliminary results on three W-bonded n-type elements held at 600°C for 500 hours were included in the First Quarterly Report. More complete results are presented here.

Three W-diffusion-bonded n-type PbTe elements were sealed under a partial pressure of argon in small, individual Vycor ampoules. One electrode had been broken from one of the elements, so values for contact resistivity represent the average of five bonds. Other values are the average of all three elements. Initial contact resistivity was 13 $\mu\Omega$-cm^2 and room temperature bulk resistivity was 0.540 mΩ-cm. After testing, contact resistivity had increased to 48 $\mu\Omega$-cm^2 (equivalent resistance: 0.15 mΩ). The increase was consistently about four times for all five bonds. Bulk resistivity decreased to about 0.500 mΩ-cm. Figure 12 shows the Seebeck voltage of the life-tested elements compared to as-bonded elements. The variation of bulk resistivity with temperature is presented in Fig. 13. The variation of total element resistance with temperature was also measured for the two whole elements. The average of the two curves coincided almost exactly with the average curve for total element resistance of as-bonded n-type. This indicates that the temperature variation of contact resistance may be somewhat decreased in the life-tested samples.

Metallographic examination showed no significant changes in the microstructures of the elements. The micrographs presented in the First Quarterly Report were representative of all three. Electron beam scans were made on one of the elements, and although the surface preparation was not optimal, there appeared to be no interdiffusion of element or electrode beyond the limited amount found in as-bonded specimens.

V. ELEMENT EVALUATION

A. Asarco PbTe

Samples of PbTe thermoelectric material produced by Asarco Intermetallics Corporation were received from the manufacturer and from Mr. Joseph Epstein of GSFC for evaluation. Samples from AIC are

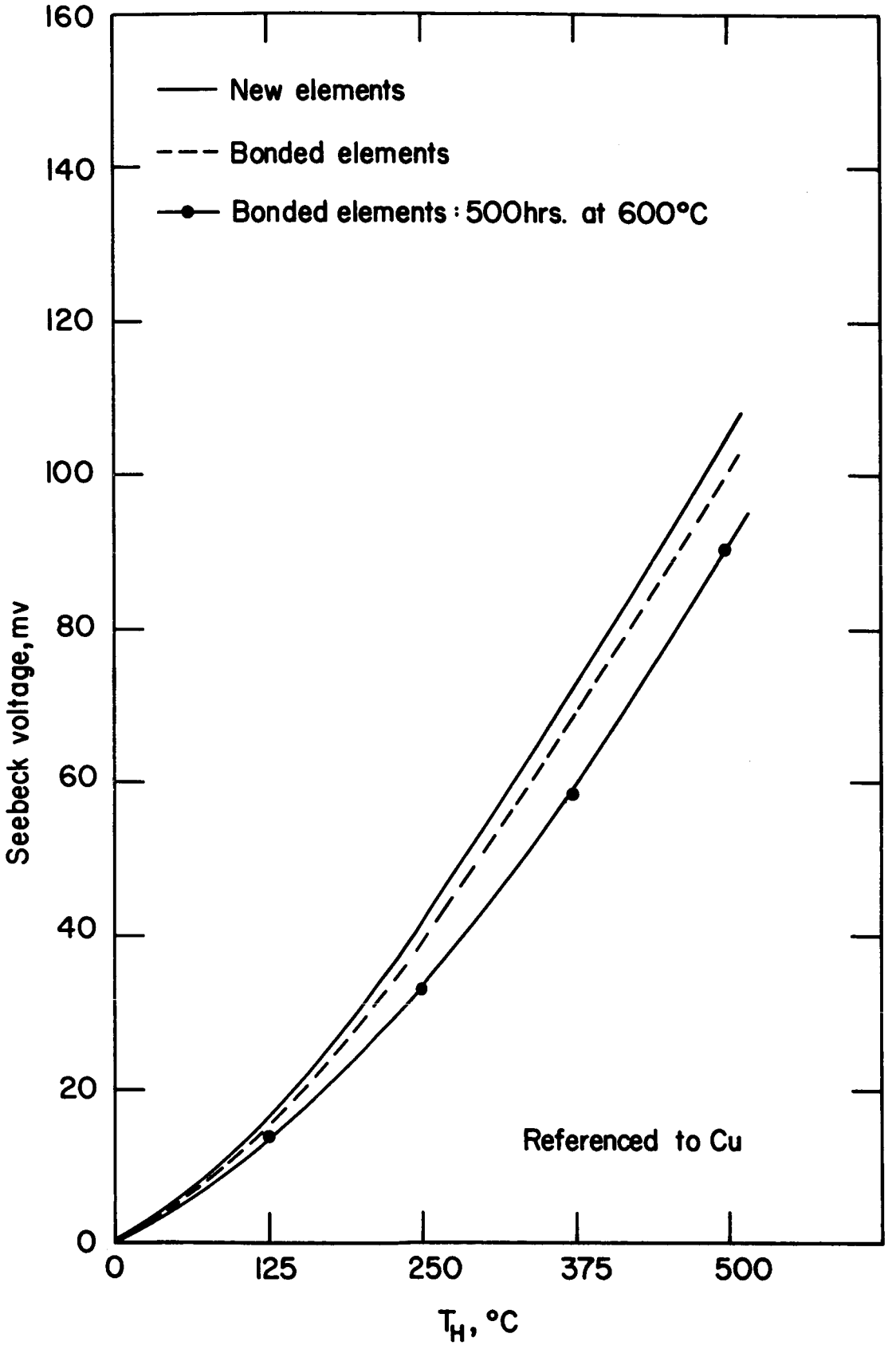

Fig. 12 Seebeck voltage of life-tested W-bonded n-type elements after 500 hours at 600°C.

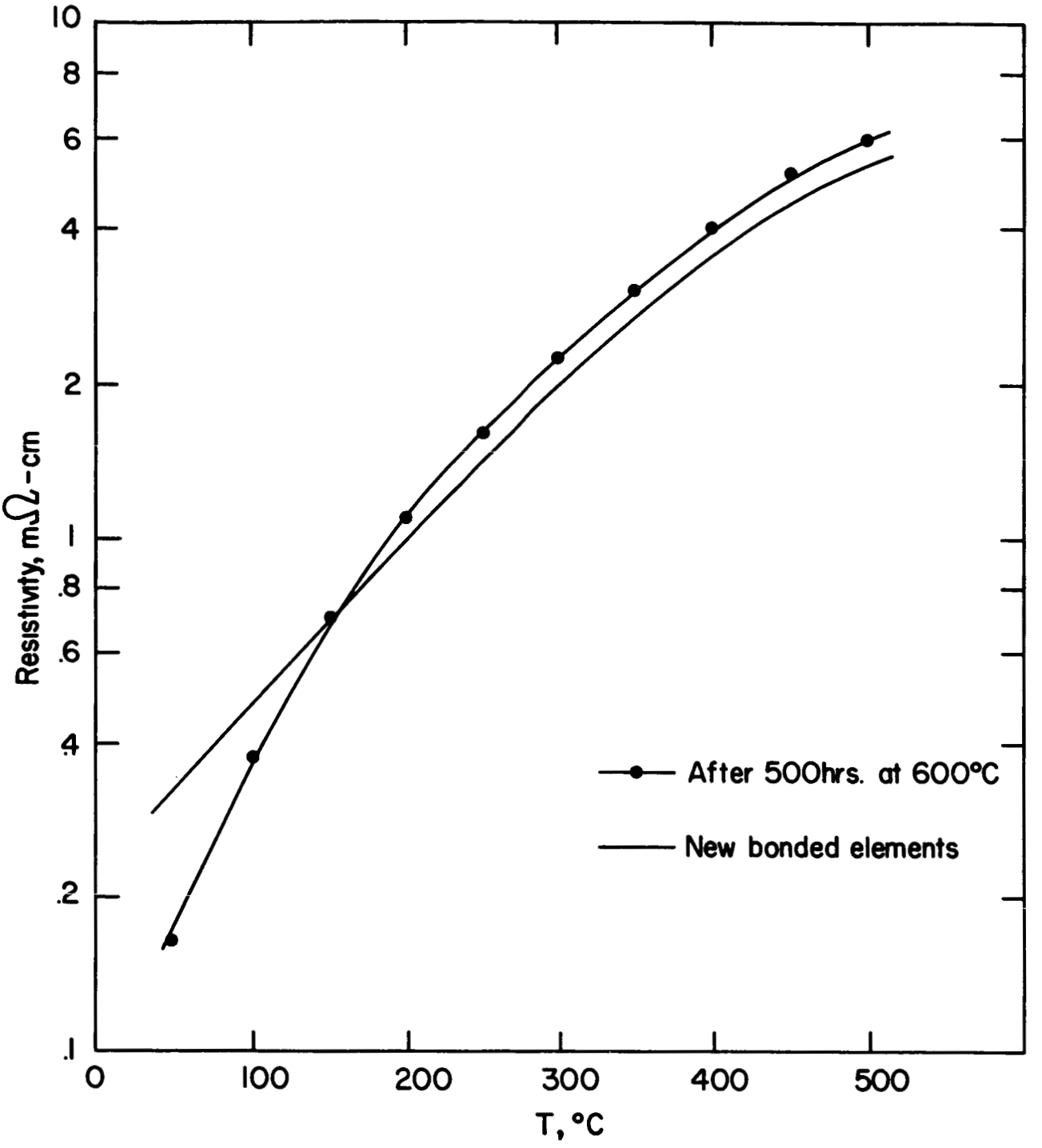

Fig. 13 Bulk resistivity as a function of temperature of life-tested n-type elements.

designated As-I and As-II, while the Epstein samples are As-1 and As-2. As-I and As-1 are p-type, the other two are n-type. Densities of these samples are listed in Table I.

TABLE I

Density and Microhardness of Asarco PbTe

Sample	Density g/cm^3	VHN (kg/mm^2)
As-I	8.54	45
As-II	8.33	34
As-1	7.82	54
As-2	7.91	56
PbTe (100% dense)	8.30	
Pb	11.34	
Te	6.25	

It is immediately apparent from the densities that the two sets of samples have been prepared differently or are of very different compositions. Since As-I and II both exceed the theoretical density of PbTe, it would be reasonable to assume that they contain substantial amounts of excess Pb, particularly As-I. However, excess Pb promotes n-type conductivity, so As-I must contain another high density p-type addition, Tl perhaps. The considerable differences in microhardness between the two sets of samples indicate that the difference between the two sets is due to composition changes. The variation of Seebeck coefficient with temperature is shown in Fig. 14; despite the physical differences the electrical properties are quite similar. Figure 15 shows the variation of resistivity with temperature. The samples received from the manufacturer have slightly higher resistivities.

The metallographic examination of these materials has not been completed. Our standard etching procedure brings out very regular pits along the grain boundaries in all the samples, and in the p-type these are

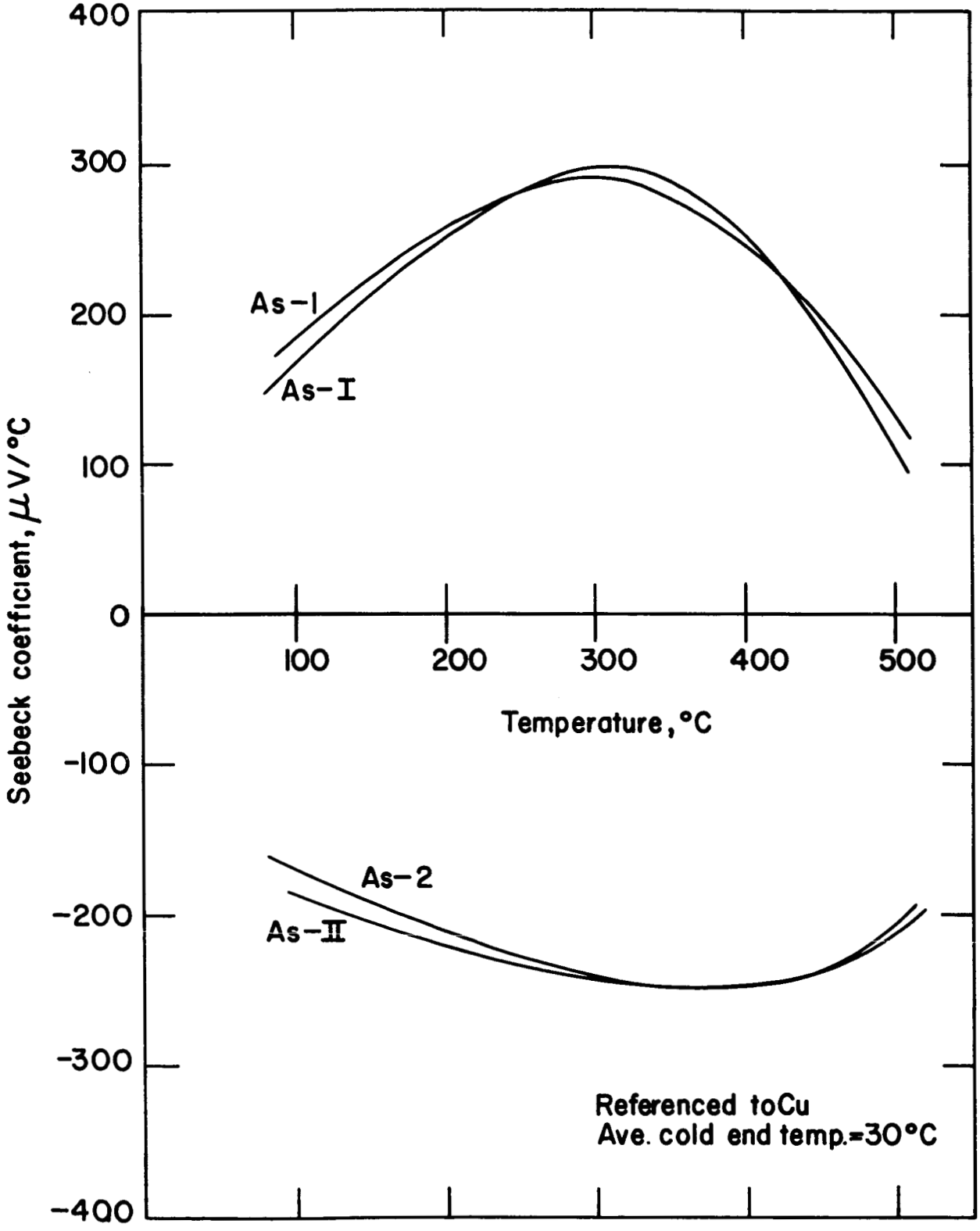

Fig. 14 Seebeck coefficient as a function of temperature for Asarco PbTe.

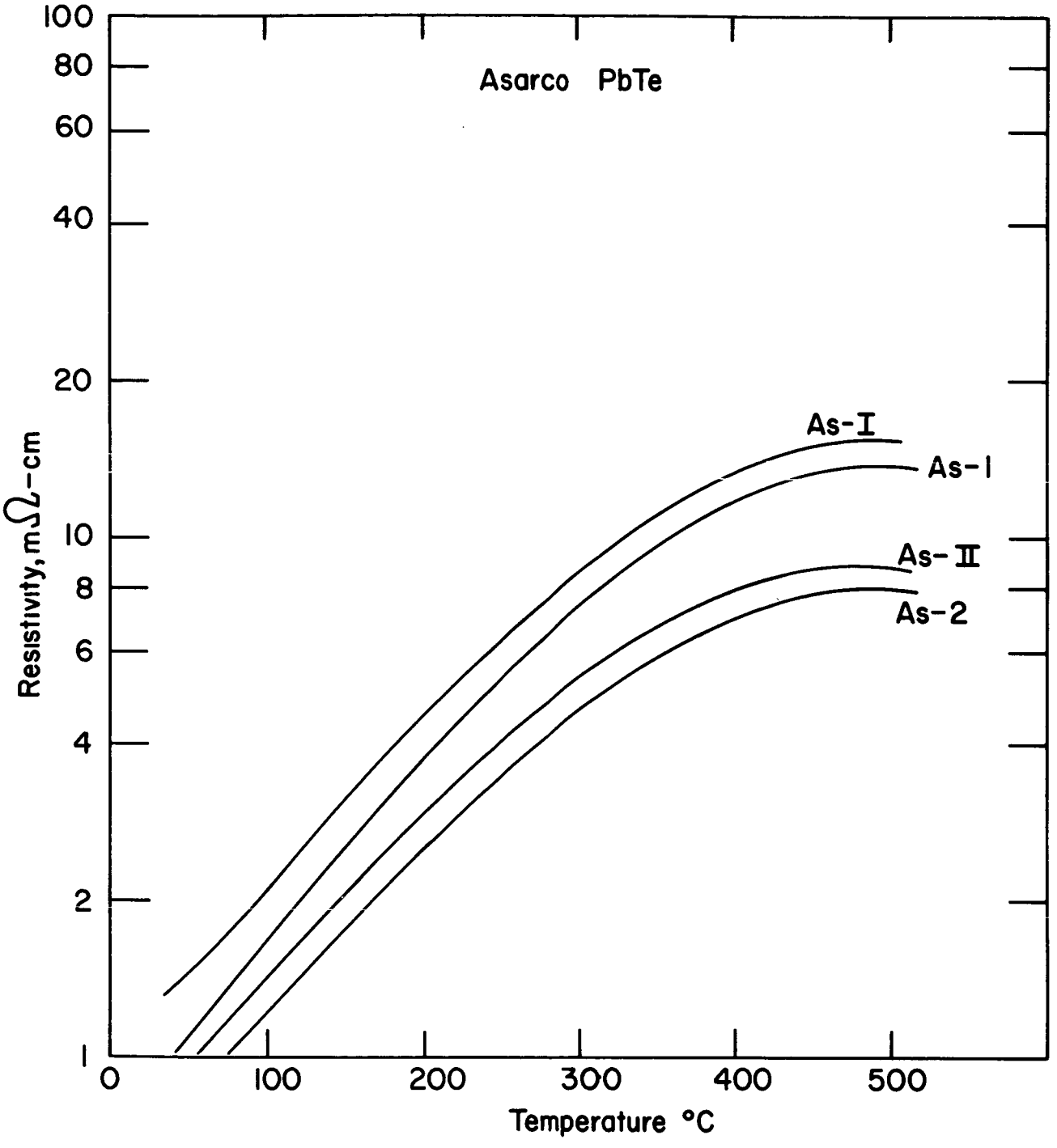

Fig. 15 Resistivity variation with temperature of Asarco PbTe.

so dense as to obscure most of the fine details of the structure. General observations indicate structures essentially the same as those found in the 3 M' s elements. Pore sizes may be slightly smaller and more uniform in size. Layering as evidenced by the arrangement of large pore-free areas termed "pseudo-grains", is very pronounced in the p-type samples. Photomicrographs will be presented in the next quarterly report.

B. Minnesota Mining and Manufacturing PbTe and $Pb_{.5}Sn_{.5}Te$

The evaluation of the 3 M' s thermoelectric materials from a number of directions has been continued. Microhardness traverses were made on n-type PbTe elements in the as-received condition and after the time-temperature cycle typically experienced by diffusion bonded n-type elements. Elements were mounted, ground to approximately the center line, and polished and etched twice before measuring. Measurements were made with a 100 g load on a Vickers diamond indenter. Traverses were made longitudinally and transversely; impressions were made at approximately 8 - 10 mil intervals. Results were virtually identical for both cases. No significant variation in microhardness from end-to-end or side-to-side was found for as-received or "annealed" elements. The average microhardness in both cases was 30.5 kg/mm^2. These measurements indicate that there are no gross variations in composition of the n-type elements, at least insofar as they might affect the microhardness of the material; and that the elements are essentially completely "annealed" after fabrication. One would not expect, in fact, any residual stresses to survive a sintering treatment, although the effects of residual or fabrication stresses which occur prior to sintering may well persist. This is apparently the case for p-type $Pb_{.5}Sn_{.5}Te$ elements which not infrequently are found to be cracked before receiving any thermal treatment at all.

The surface area of a new p-type $Pb_{.5}Sn_{.5}Te$ element was measured by the BET technique, which involves the measured adsorption of a monolayer of krypton on the sample over a range of pressures. The technique is generally applied to catalysts and other materials of high surface area, and is capable of quite high precision. The sample which was measured

had a geometrical surface of 1.54 cm^2 , while the measured surface area was 405 cm^2. Two n-type and another p-type element will be measured during the next quarter to try to gain a better idea of the significance of this number and how it relates to the different behavior of the two types of material. A rough calculation of the double layer coverage of the average amount of oxygen found in p-type elements gives about 70 square meters. This would indicate that the major part of the oxygen present is dissolved or present as oxides, when compared to the surface area measured, even though this represents only the surface accessible to the outside, and not the total surface of all internal pores.

Vacuum fusion gas analyses have, at present, been done for eight p-type elements and two n-type elements. The average oxygen content for six new p-type elements which are from three separate lots of elements is 435 ppm; the nitrogen content is 10 ppm. Two other elements which were measured after diffusion-bonding had an average oxygen content of 320 ppm and a nitrogen content of 10 ppm. The average oxygen content of the two n-type elements (new) was 80 ppm; no nitrogen was found. A 1962 report by Westinghouse[4] lists gas contents of two heats of n-type PbTe from pure elements to finished pellets. Oxygen in the Pb and Te is about 20 ppm; after reaction and casting the PbTe had about 60 ppm. Jaw-crushing to powder raised the oxygen to about 340 ppm. The powder was then reduced in hydrogen, pressed, and sintered in argon to give a final oxygen level in the fabricated elements of about 175 ppm, and a nitrogen level of about 100 ppm. These results give support to the oxygen levels measured in our elements as being realistic, although far from desirable.

VI. CONCLUSIONS

The major effort during this quarter was directed toward the definition of a satisfactory bonding system and process for p-type $Pb_{.5}Sn_{.5}Te$, and the design of the life test device. The following conclusions may be made from these studies:

1. The use of SnTe braze to bond W or Ta electrodes to $Pb_{.5}Sn_{.5}Te$ causes extensive cracking in the bulk of the thermoelement.

2. Diffusion bonding of W to $Pb_{.5}Sn_{.5}Te$ appears to be a feasible method.

3. Measurements of n-type W-bonded elements held at 600° for 500 hours showed an increase in average contact resistivity from 13 to 48 $\mu\Omega$-cm^2. Seebeck voltage decreased slightly and bulk resistivity increased slightly above as-bonded over 200°C.

4. Electron beam microprobe studies of as-bonded W-diffusion bonds to n-and p-type elements show a shallow diffusion zone about 2 microns thick, with no evidence of compound formation.

VII. FUTURE WORK

In the next quarter the following areas will be covered:

1. Thorough evaluation of W diffusion bonding to $Pb_{.5}Sn_{.5}Te$.

2. Preparation and testing of bonded n-type and p-type elements at elevated temperatures and under thermal gradient cycling.

3. Further study of contact resistance variation with temperature for n-and p-type.

4. Continued evaluation of physical and chemical characteristics of thermoelements.

VIII. REFERENCES

1. Y. Ukrainskii, A. Novoselova, and Y. Simanov, Zhur. Neorg. Khim., 4, 148 (1959). CA, 53, 12084b (1959).
2. L. Brixner, in Chemical and Thermodynamic Properties at High Temperatures, XVIII Int'l Cong. of Pure and App. Chem., Montreal, 1961, p. 202.
3. Thermoelectric Bonding Study: Summary Report, Hittman Associates, Inc., Contract No. NAS 5-3973, 1965.
4. Thermoelectricity, Quarterly Progress Report No. 1, Westinghouse Electric Corp., Contract NObs-86595, AD 283 656.
5. Japan Electron Optics, courtesy of Fisher Scientific Company, Medford, Massachusetts.

APPENDIX

DETAILED DESCRIPTION OF MULTI-STATION LIFE TEST DEVICE

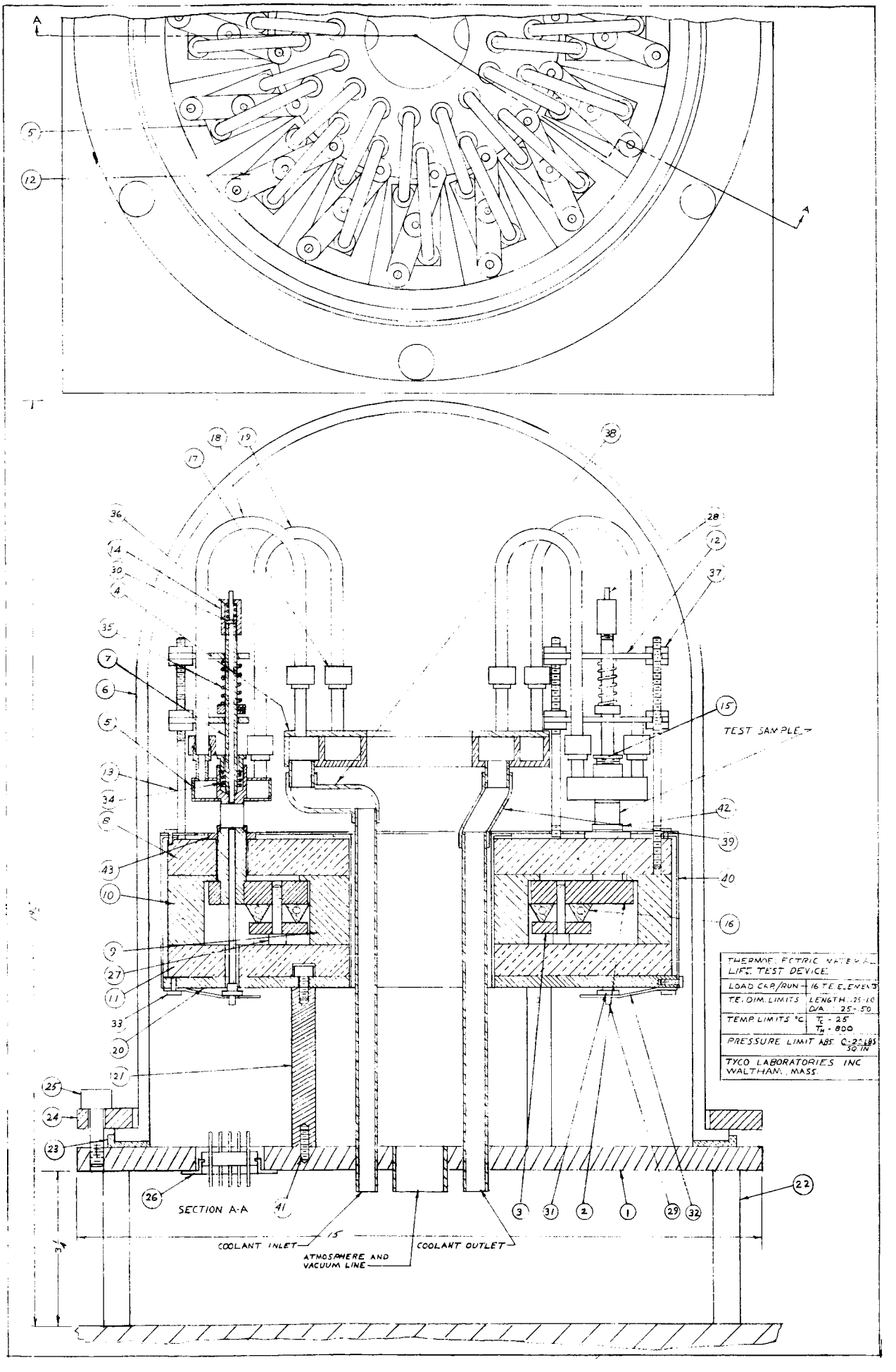
A
A
5
12
18
19
17
38
36
14
30
4
35
7
6
5
13
34
8
43
10
9
27
11
33
20
21
25
24
23
26
SECTION A-A
41
28
12
37
15
TEST SAMPLE
42
39
40
16
22
3
31
2
1
29
32
COOLANT INLET
15
ATMOSPHERE AND VACUUM LINE
COOLANT OUTLET
THERMOELECTRIC NATE V-A LIFE TEST DEVICE
LOAD CAP/RUN — 16 T.E. ELEMENTS
T.E. DIM. LIMITS — LENGTH .25-.10 DIA .25-.50
TEMP LIMITS °C — T_c - 25 T_h - 800
PRESSURE LIMIT ABS. C-2 LBS/SQ IN
TYCO LABORATORIES INC WALTHAM, MASS.

Fig. 1

APPENDIX

DETAILED DESCRIPTION OF MULTI-STATION LIFE TEST DEVICE

A detailed cross-sectional view and plan view of the life-testing device are shown in Fig. 1. Figure 3 is a schematic block diagram of the switching and measurement apparatus. Detail drawings of most of the parts requiring machining follow Fig. 3. A parts list of the mechanical assembly is included after the detail drawings.

1. Mechanical Assembly: A test specimen is shown in position on the right-hand side of Fig. 1. The specimen is centered by a retaining ring, 42. Heat is supplied to the bottom of the specimen through the individual studs brazed to the heater ring, 2. The heating elements, 16, are clamped tightly against the ring by 3. The hot junction thermocouple, shown in the section on the left, is held in place by the spring and spring plate, 32 and 31. Insulation is provided for the heater ring assembly by pieces of machined, fired lavite, 8, 9, 10, 11. This assembly is supported by the plate, 20, and shielded by a thin metal casing, 40. The individual cold junction assembly is held by the support rods, 13. Vertical adjustment is provided by the bearing plates, 12, and nuts, 37. The water-cooled cold junction block, 5, is free to rotate about the end of the pressure rod, 7, to allow for alignment with nonparallel specimen ends. Pressure on the element, from the heat sink is provided by the spring, 35. This pressure is adjustable. Water flows completely around the central stud in the heat sink. Pressure on the cold end thermocouple is provided by the spring, plate, and nut assembly, 36, 30, 14, at the upper end of the pressure rod.

Flexible tubing, 18, 19, supplies and exhausts cooling water to the heat sink. Connections to the water manifold, 4, are parallel so that all the cold junctions receive water of the same temperature. The heater assembly is electrically common to all the elements, but isolated from the rest of the system. The individual heat sinks are completely isolated.

Terminal blocks will be provided for all thermocouple connections inside the system in the space under the heater assembly; thus leads through the vacuum-tight fittings (Conax) in the base plate, 1, need be installed only once.

2. Electronics: The heater assembly will impose a common ground on the electrical testing connections. Each element will have, in addition, to the heater contact, a thermocouple at each end of the element (A_1-C_1 and A_2-C_2) and an individual, electrically isolated, cooling contact on the cold side (M_2), (see Fig. 2).

The testing of each element for the four desired characteristics will involve measurement of the following:

1. The temperature at the hot end, T_h, will involve measurement of a d.c. potential of the order of 10's of mvs between A_1 and C_1.
2. The temperature at the cold end, T_c, will involve d.c. measurement of the order of a mv between A_2 and C_2.
3. The thermoelectric emf under open circuit is a d.c. potential of the order of 10's of mv between A_1 and A_2 or C_1 and C_2.
4. The determination of the internal impedance (resistance) of the thermoelement will be performed by forcing approximately one ampere of 100 cps a.c. current from M_2 to M_1 and measuring the a.c. voltage between A_1 and A_2 or C_1 and C_2. This will add to the thermoelectric d.c. potential an a.c. component of the order of one to five mv.

The approach to these measurements will be the use of one high quality, floating input d.c. millivoltmeter preceded by a high quality thermoelectric type mechanical switching network to select the contacts from one thermoelement at a time. This switching network is also equipped with an electro-mechanical activator to provide automatic switching sequence when desired.

A second, similar switching network follows the above network and is used to select the above outlined four tests in sequence.

The millivoltmeter can read the output directly in digital form; the Digitec instruments are ideal units for this purpose. Provision is also made to read these instruments electronically and thereby provide digital drive for a printer unit which would print the test measurements along with identification data for each test point. A digital punch device is also available to provide an output form directly designed for computer assimilation. For the a.c. resistance test, the d.c. millivoltmeter is preceded by a precision a.c. to d.c. converter. Figure 3 is a schematic block diagram of the thermoelectric testing electronics.

In addition to the above testing electronics, an electronic temperature controller will be required to maintain the heater at $\pm 0.5°C$ or better stability.

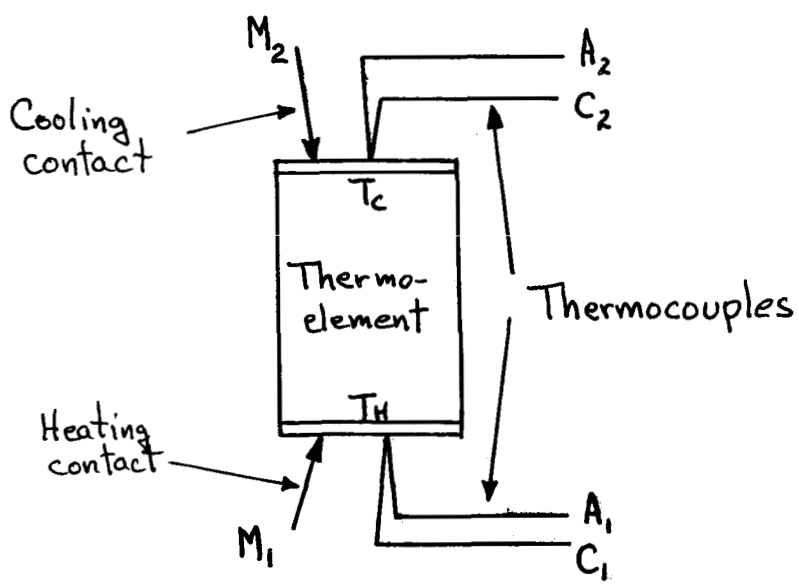

Figure 2

Fig. 3 · Schematic Block Diagram of Thermoelectric Testing Electronics

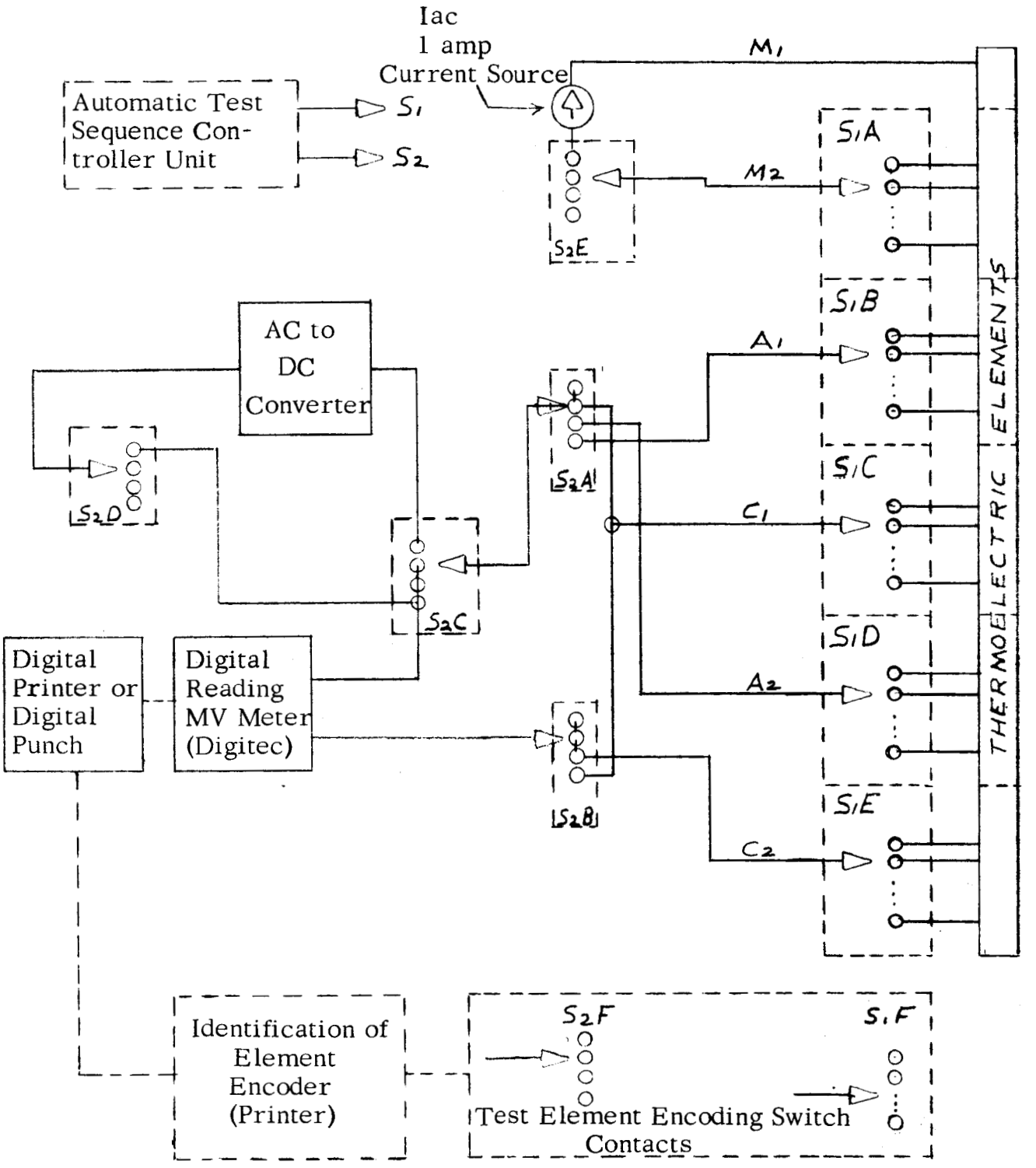

S_1 is a switch used to select the element test station.

S_2 is a switch used to sequence the four test points per station.

ESTIMATED COST FOR PROTOTYPE OF A THERMOELECTRIC TEST STATION

LABOR

	Hours	Rate	$
System Assembly and Test	$ 500	$ 4.00	$ 2,000
Electronic Component Fabrication and Test	125	4.00	500
			$ 2,500

MATERIALS

a. Machining of Metal and Ceramic Components		$2,500	
b. Electronic Equipment and Components			
1) Digitec millivoltmeter with BCD outputs	$ 590		
2) Voltmeter ranging and other modifications	210		
3) Voltmeter AC-DC converter	325		
4) Two 6-pole switches	400		
5) Special constant current source-parts	100		
6) Special controller and timer-parts	100	$1,725	
c. Automatic Data Handling Setup			
1) Digital Printer	$ 750		
2) Electronic Readout with tape punch	2,000	$2,750	
d. Auxiliary Equipment			
1) Stepless Temperature controller	$ 550		
2) Vacuum Pump	235		
3) Bell Jar	130		
4) Miscellaneous, including			
Conax Fittings Panel Rack Heating Elements Thermocouple Wire and Insulators Water Pressure Gauge and Regulator Tubing and Connectors Springs Terminal Blocks Hardware	1,085	$2,000	$ 8,975
TOTAL COST			$11,475

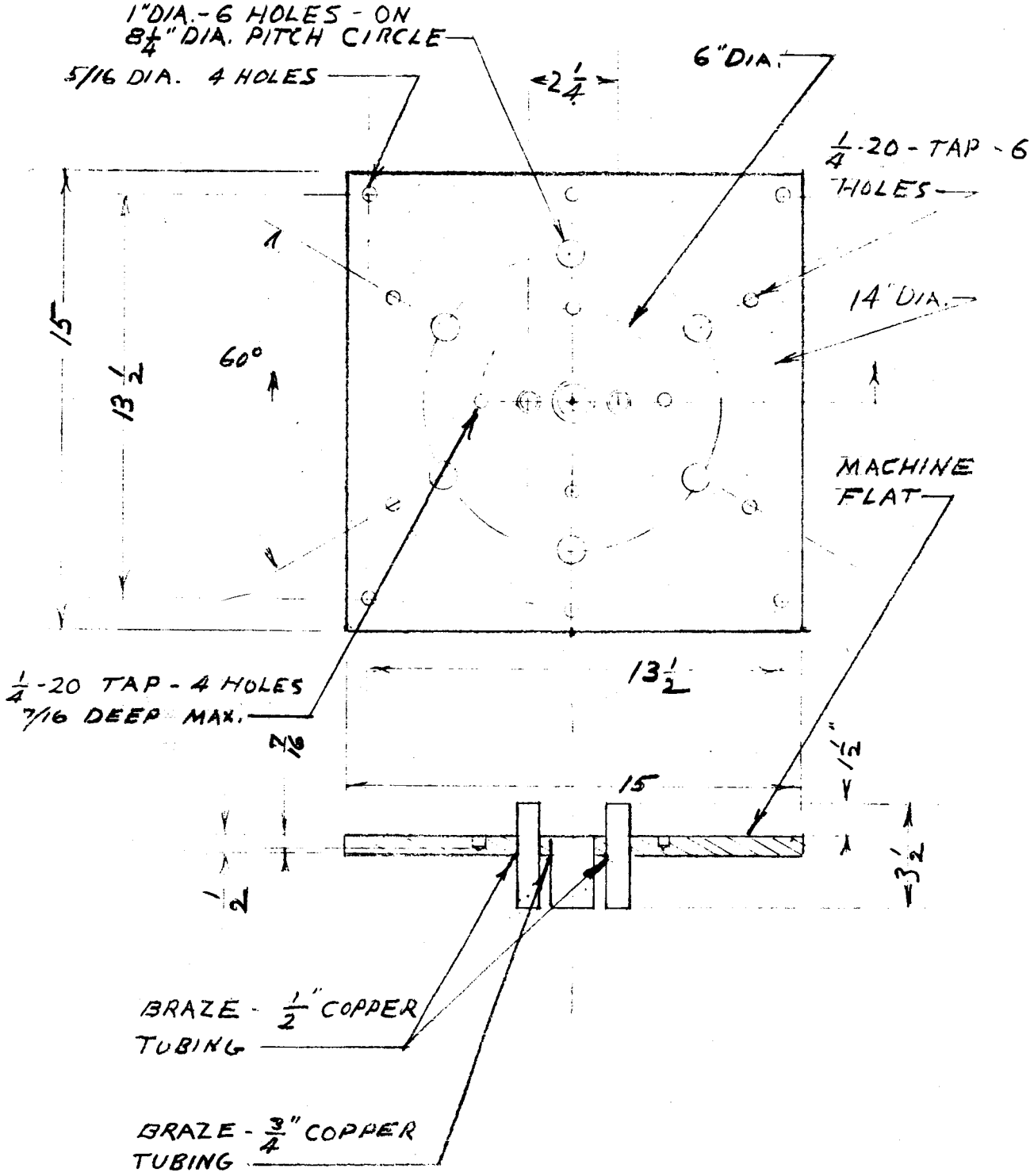

MATERIAL : 302 ST. ST.
PCS. REQ'D: 1

Pt. 1

BASE PLATE -
PROJECT NO. C-567
TYCO LABORATORIES INC.
WALTHAM, MASS.

HEATER RING

PROJECT NO. C-567

TYCO LABORATORIES INC.
WALTHAM MASS.

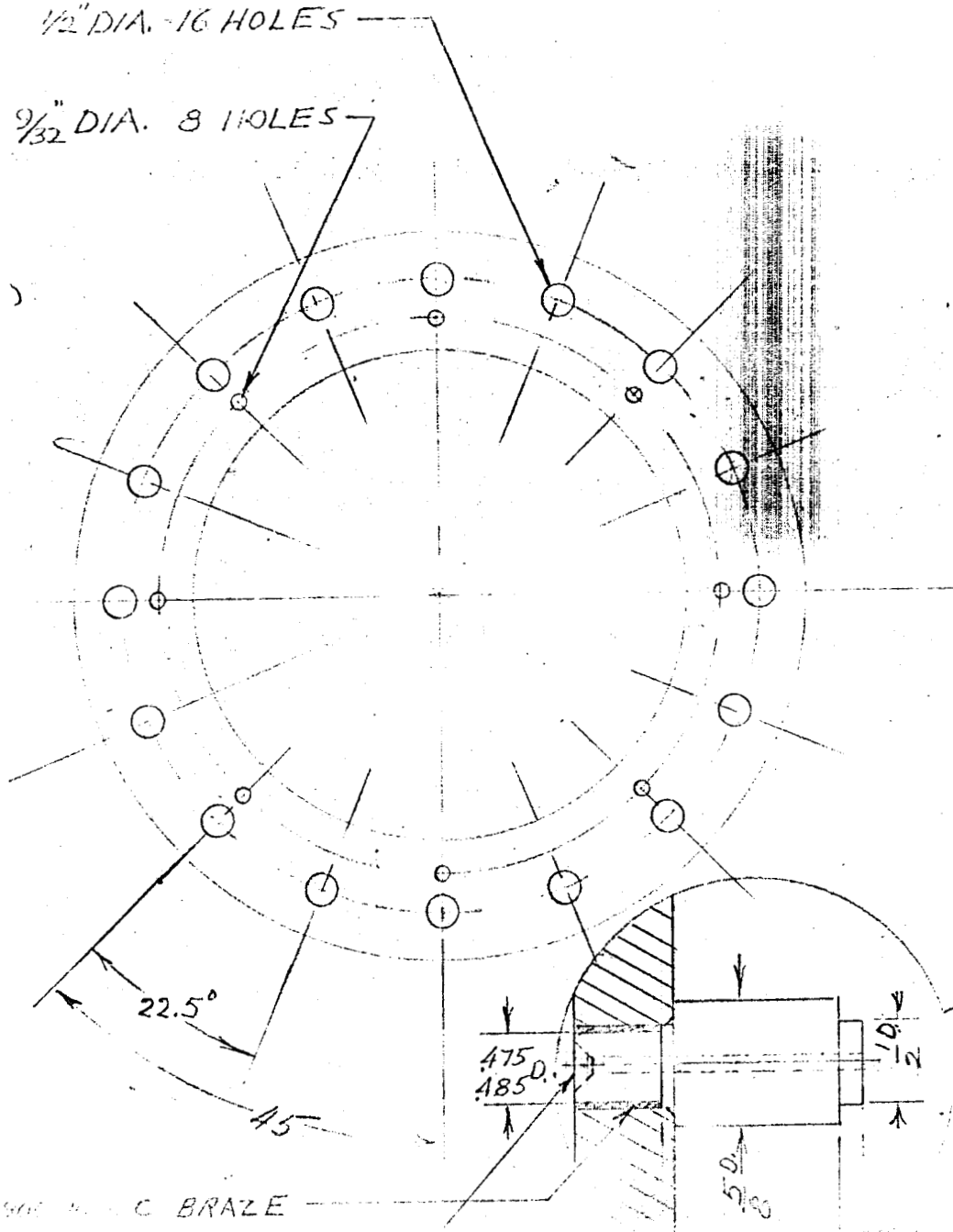

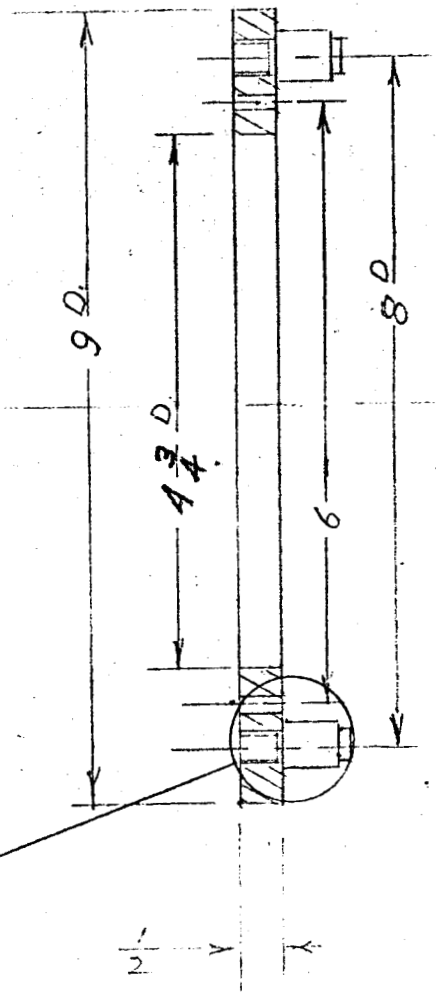

C BRAZE

MATERIAL 302 ST. ST.

PC'S. REQ'D. 1

PG. 2

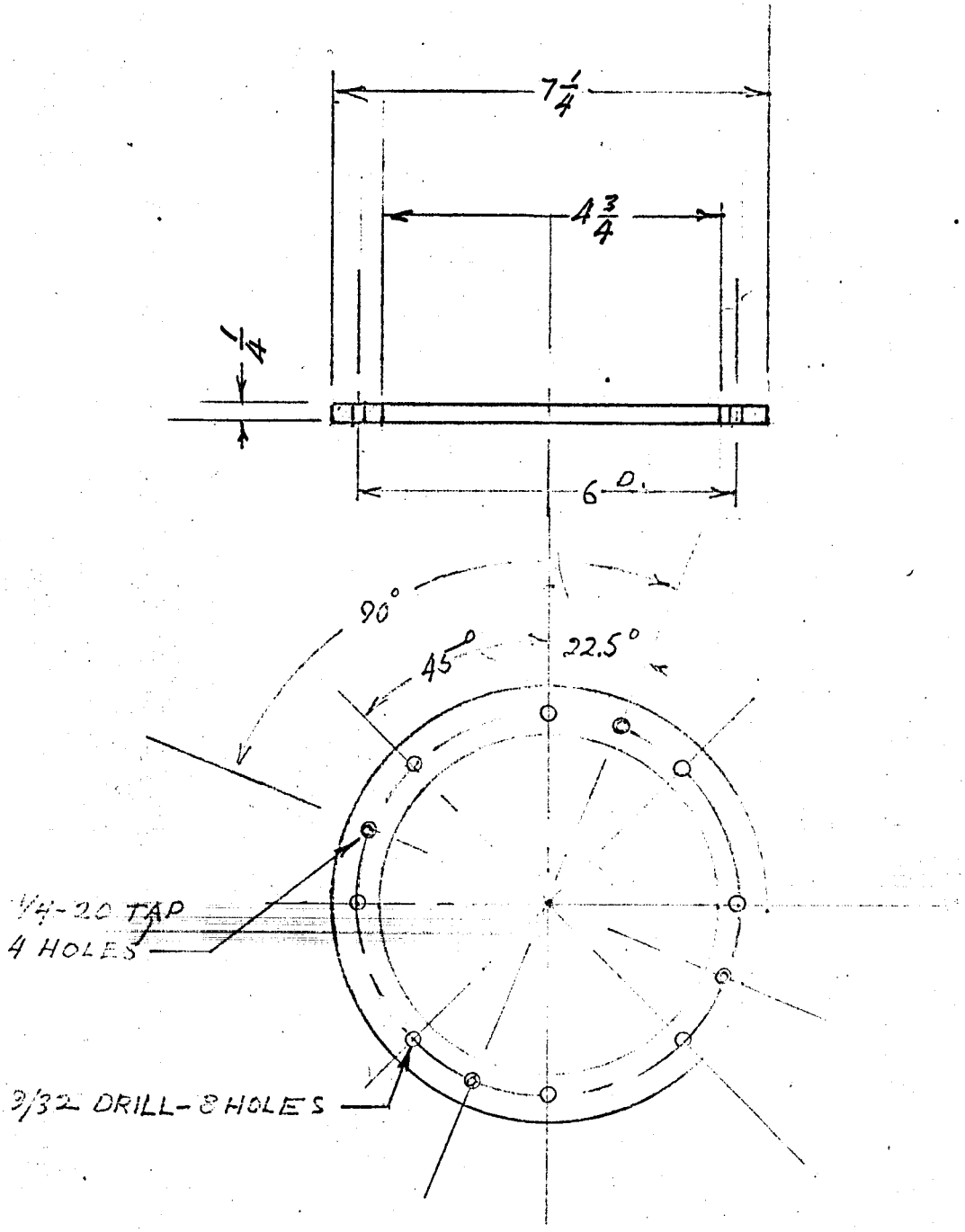

MATERIAL: ST. ST. 302
PCS.: 1

Pt. #3

HEATER RING CLAMP
PROJECT NO. C-567
TYCO LABORATORIES INC.
WALTHAM, MASS.

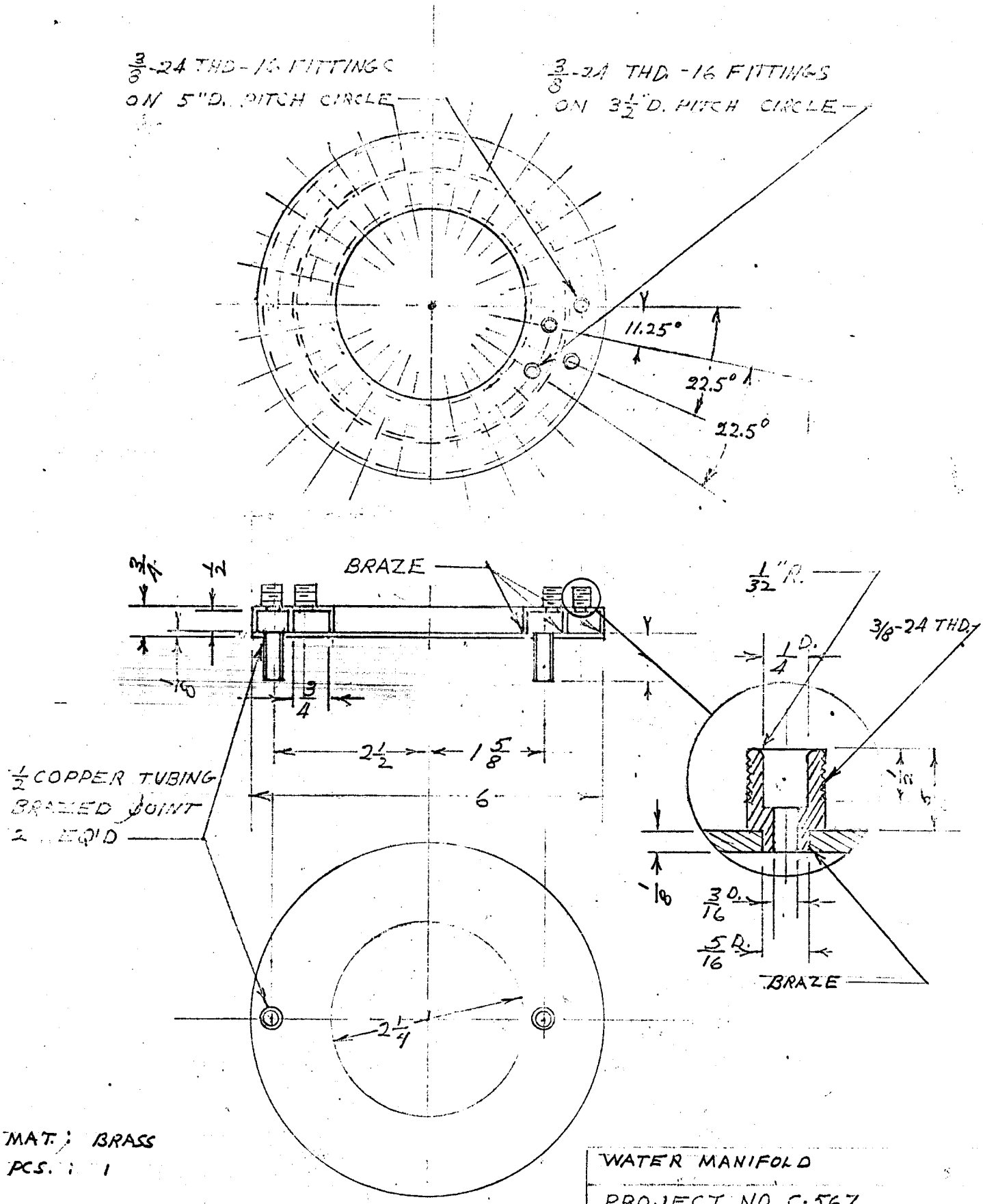

MAT.: BRASS
PCS.: 1

Pt. 4

WATER MANIFOLD
PROJECT NO. C-567
TYCO LABORATORIES INC.
WALTHAM, MASS.

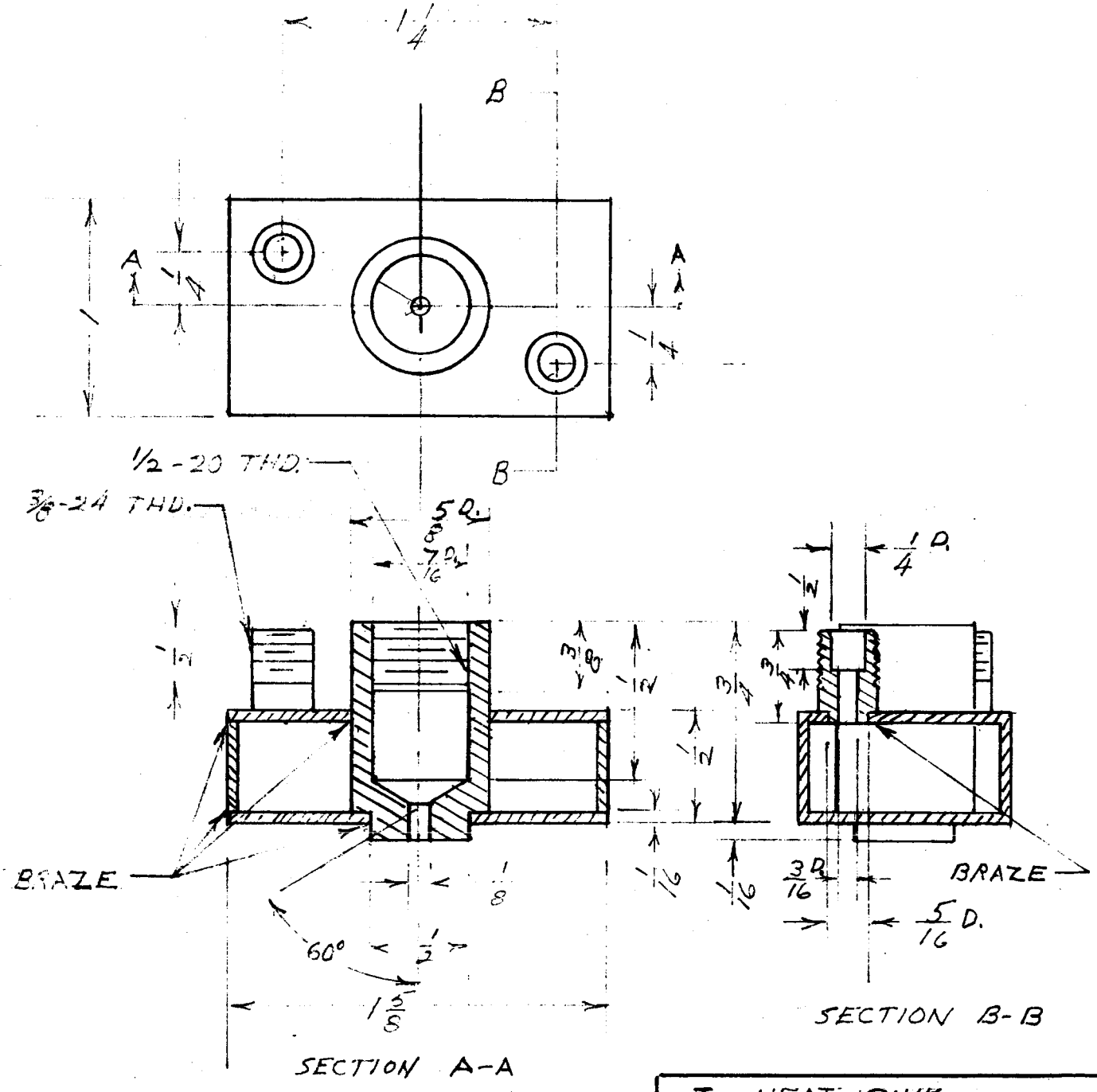

MATERIAL : COPPER
PCS. : 16

Pt. 5

Tc HEAT SINK
PROJECT NO. C-567
TYCO LABORATORIES WALTHAM, MASS.

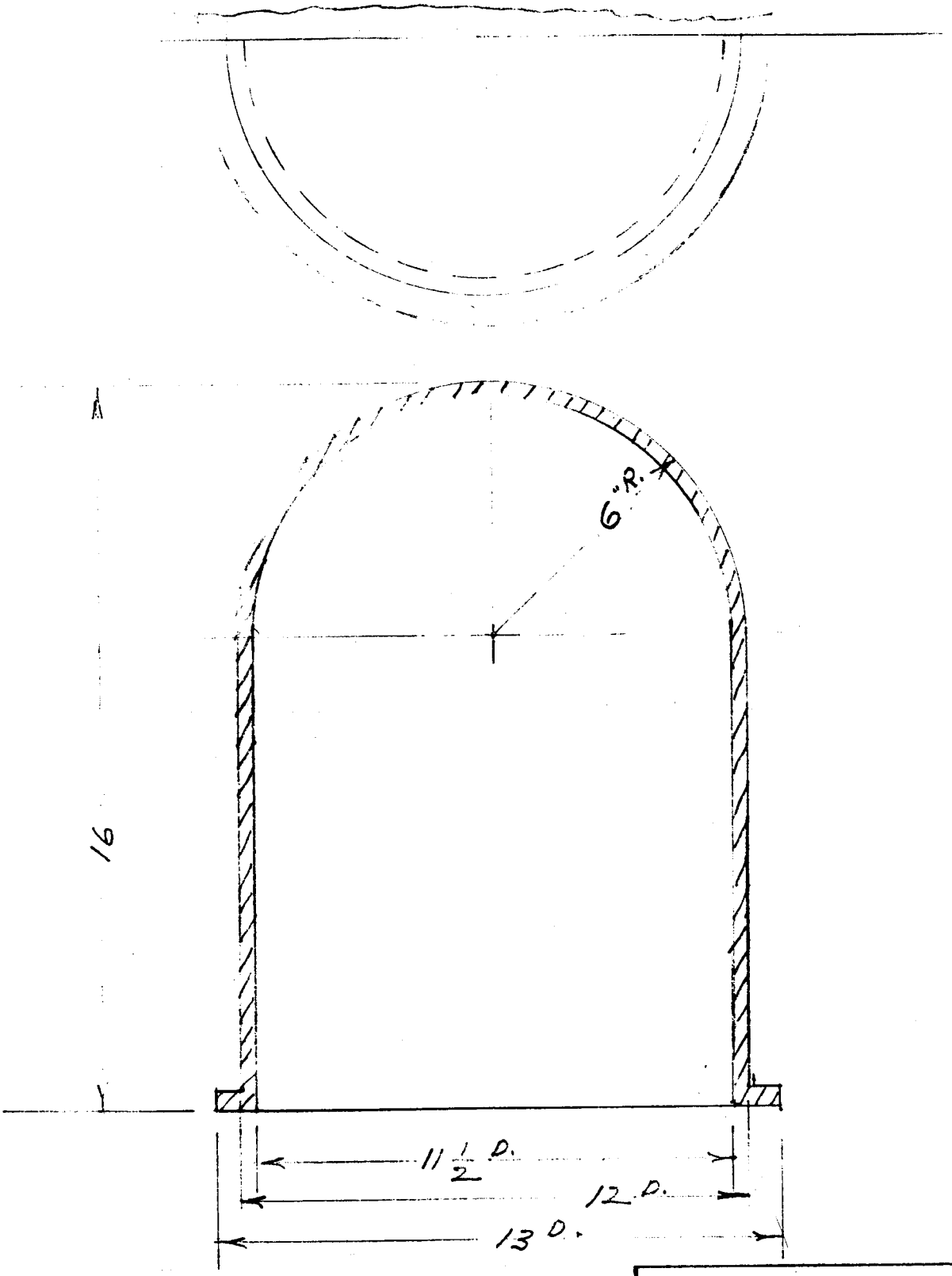

MAT. : PYREX GLASS
PCS. REQ'D : 1

Pt. 6

BELL JAR
PROJECT NO. C-567
TYCO LABORATORIES INC. WALTHAM, MASS.

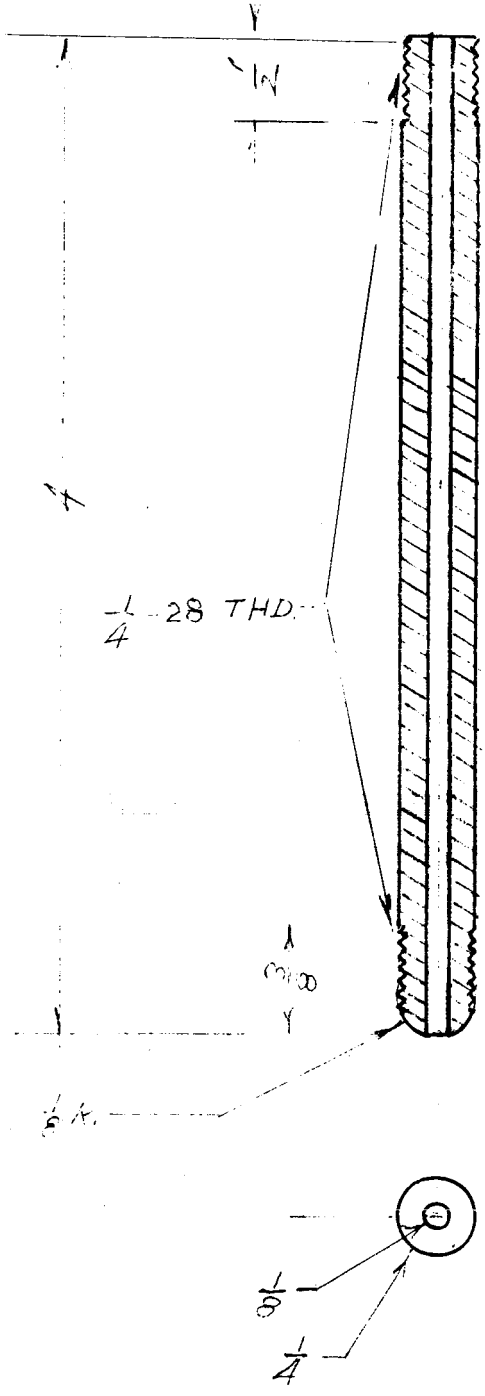

MAT. : 302 ST. ST.

PCS. : 16

Pt. #7

PRESSURE ROD.
PROJECT NO. C-567
TYCO LABORATORIES INC.
WALTHAM, MASS.

THERMAL INSULATOR TOP

PROJECT NO. C-567

TYCO LABORATORIES INC.
WALTHAM MASS.

MAT. : FIRED LAVA

PCS. REQ'D : 16

Pt. 8

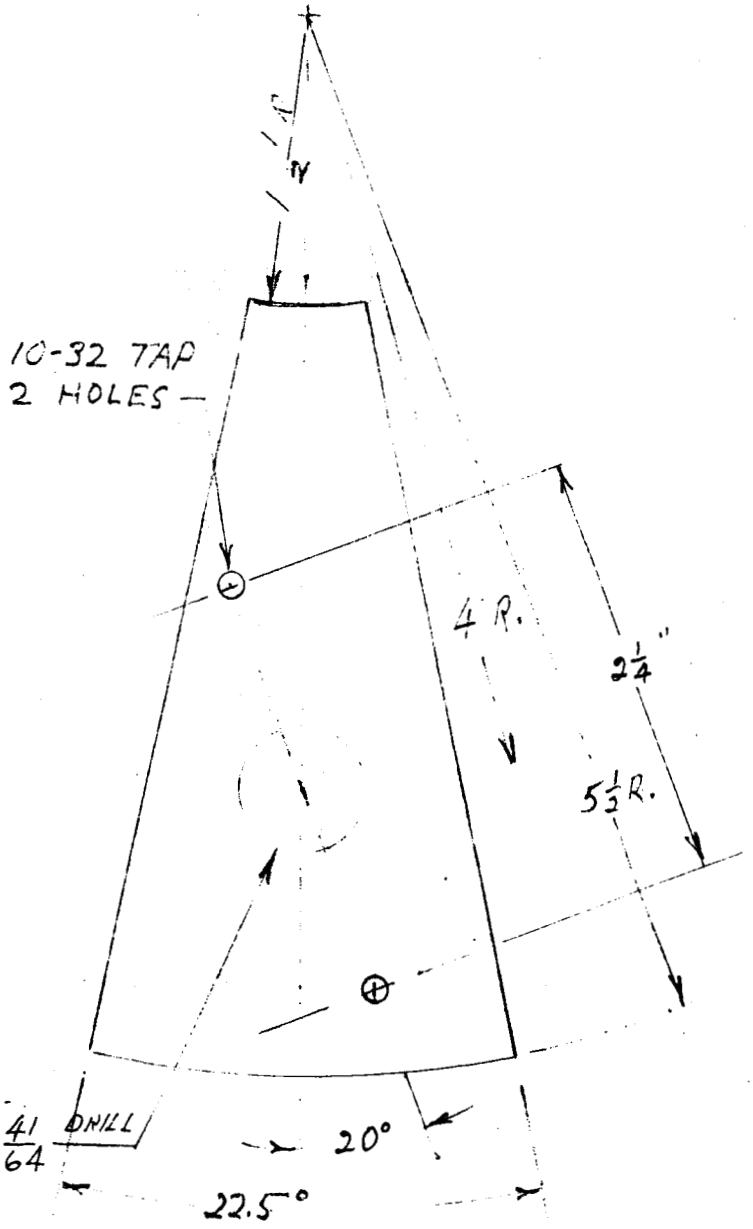

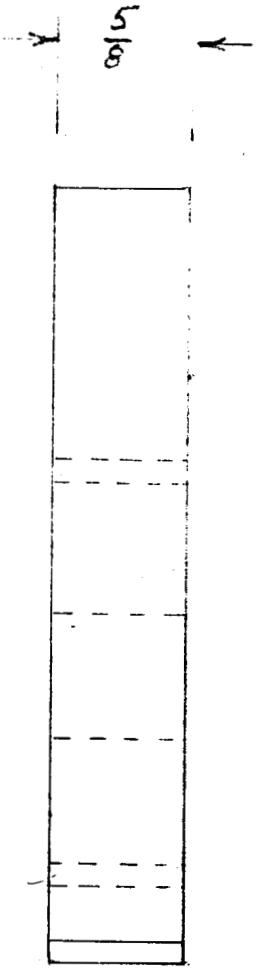

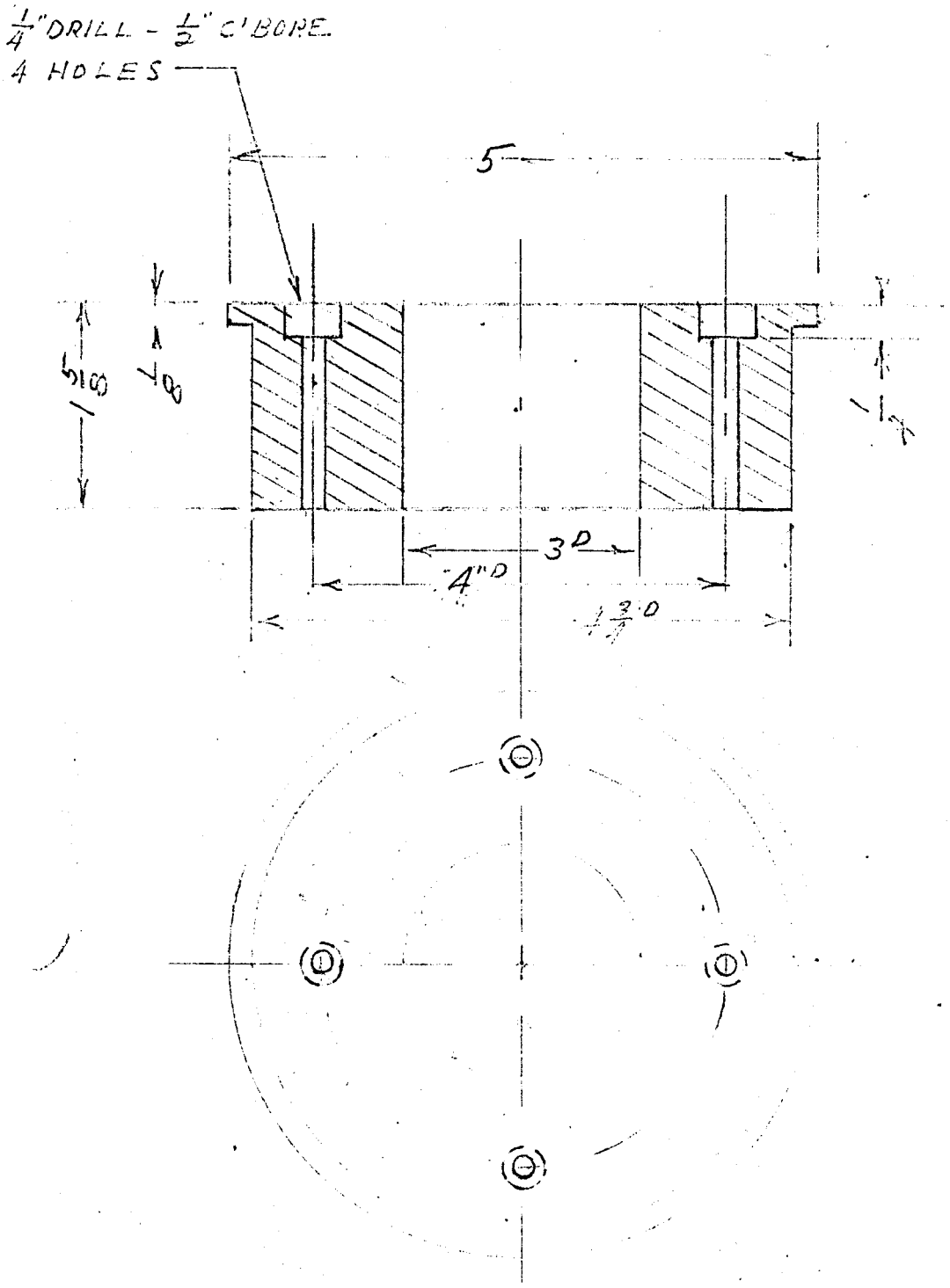

MATERIAL : FIRED LAVA

PCS. REQ'D: 1

PL. 9

THERMAL INSULATOR-INSIDE
PROJECT NO. C-567
TYCO LABORATORIES
WALTHAM, MASS.

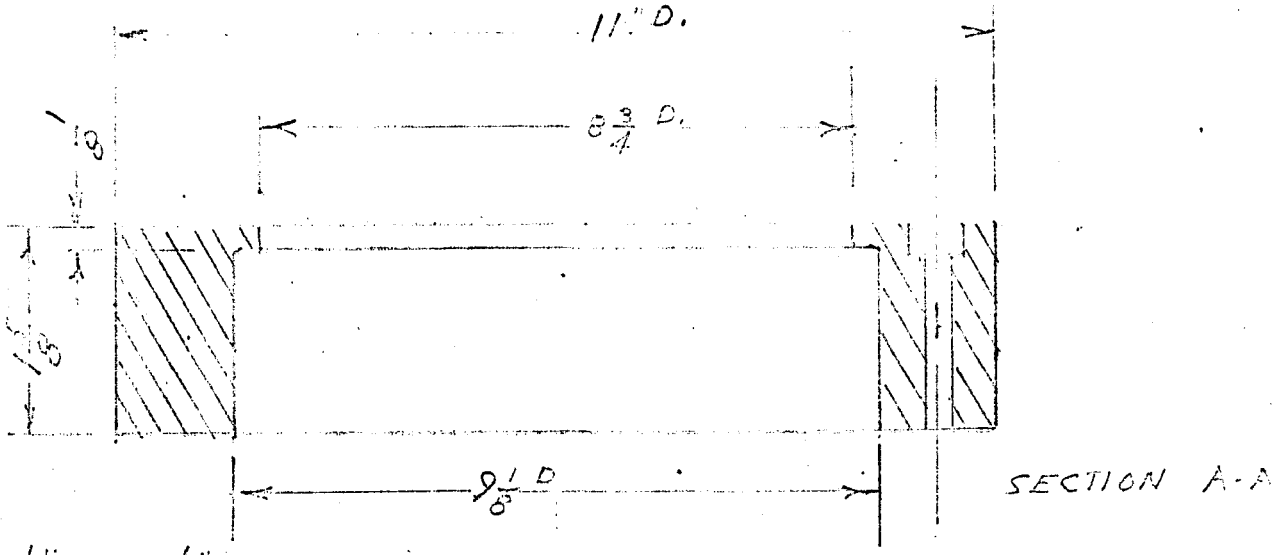

SECTION A-A

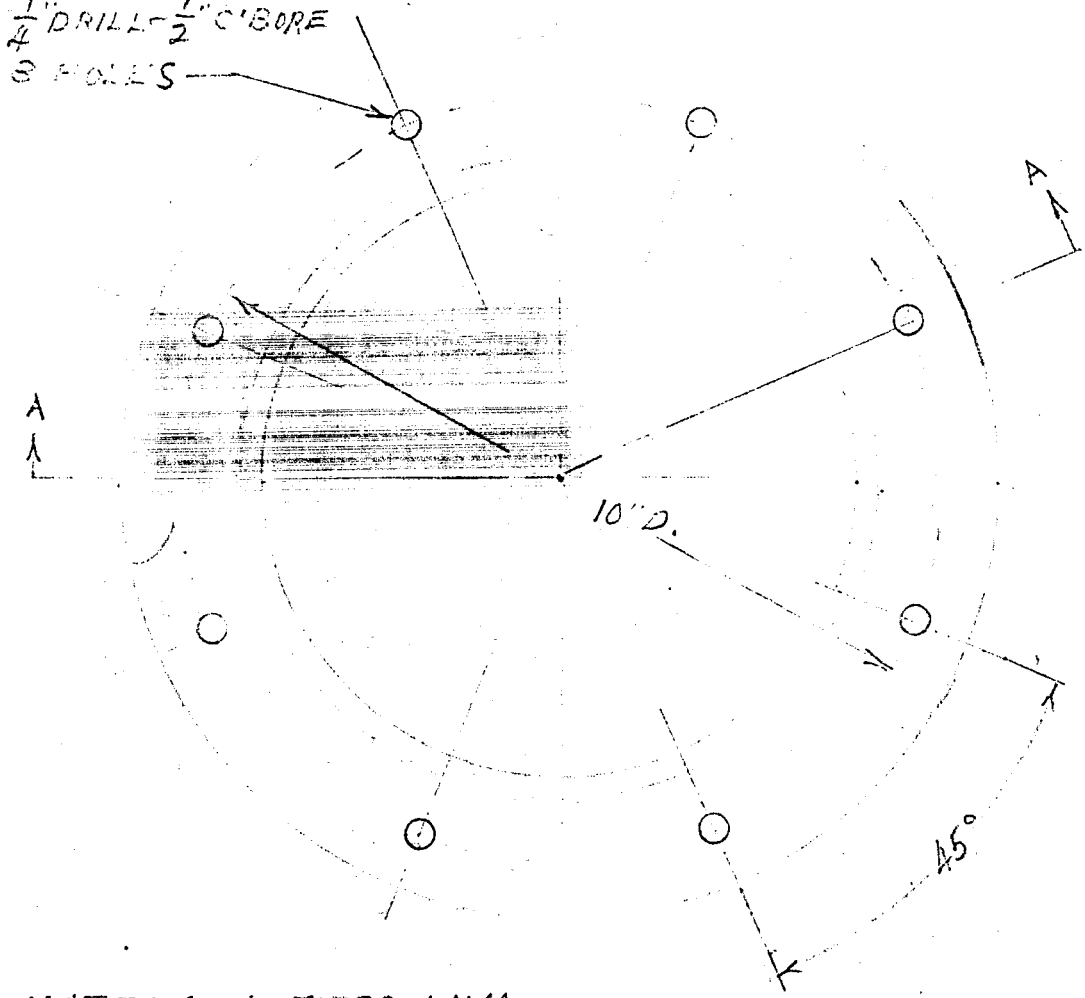

MATERIAL : FIRED LAVA

PCS. REQ'D : 1

(10)

THERMAL INSULATOR - 5"
PROJECT NO. C-567
TYCO LABORATORIES INC. WALTHAM MASS.

THERMAL INSULATOR-BOT.

PROJECT NO. C-567

TYCO LABORATORIES INC.
WALTHAM, MASS.

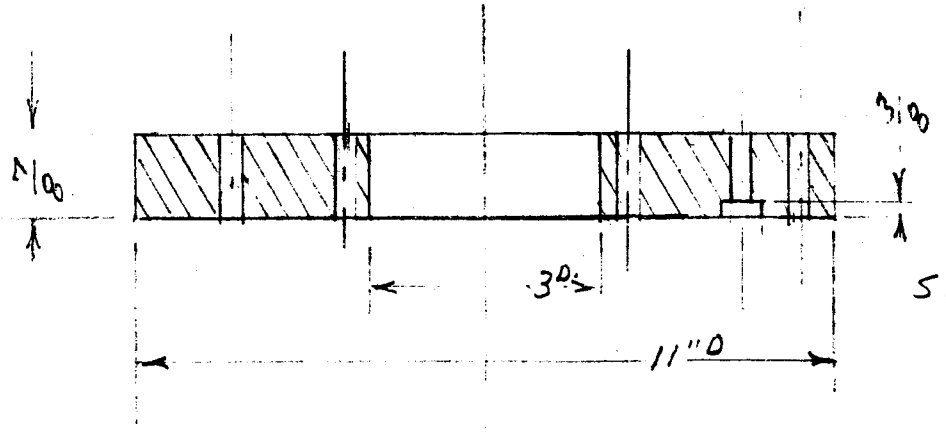

SECTION A-A

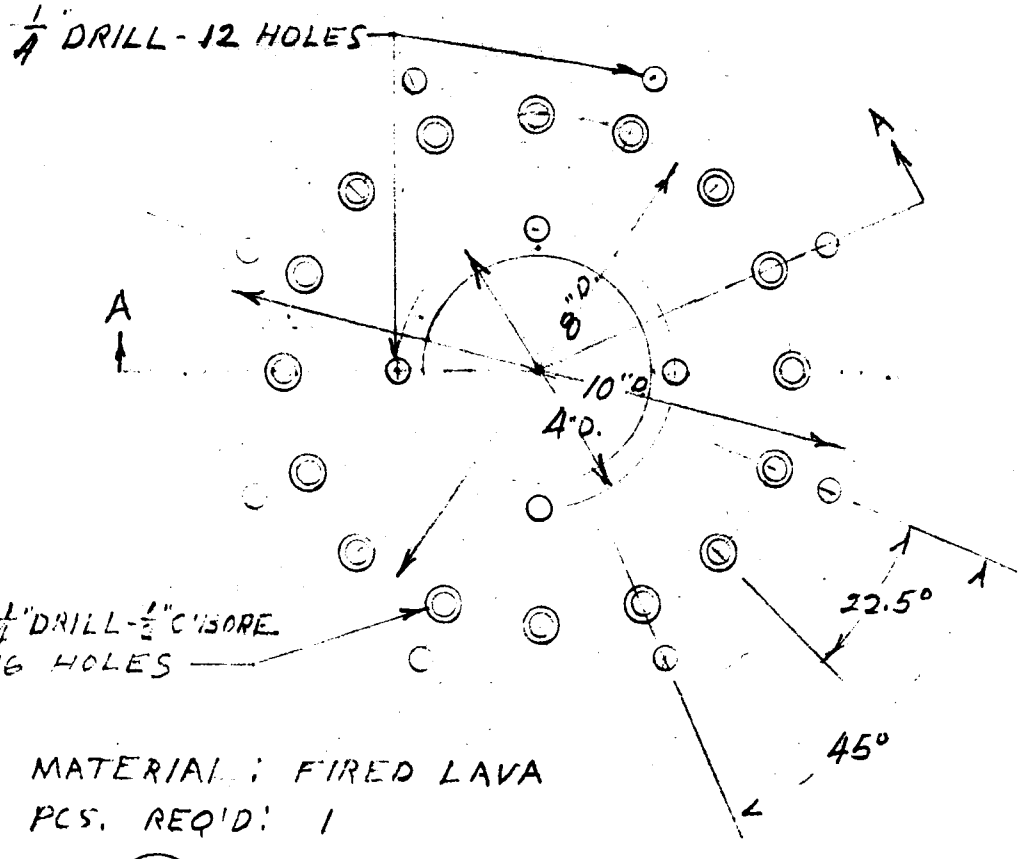

MATERIAL : FIRED LAVA
PCS. REQ'D: 1

(11)

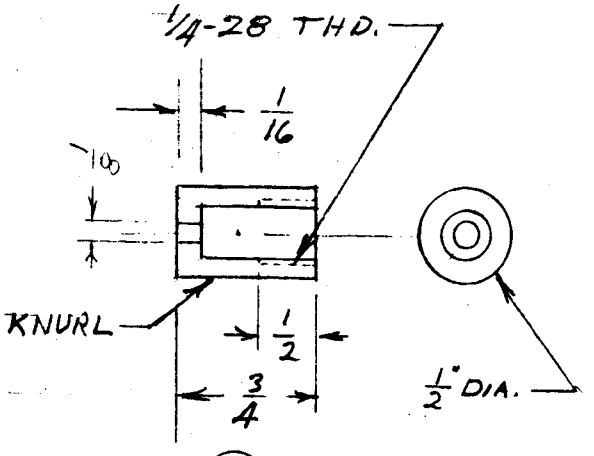

Pt. # (14) TC SPRING NUT
MAT. 302 ST. ST.
PCS. 16

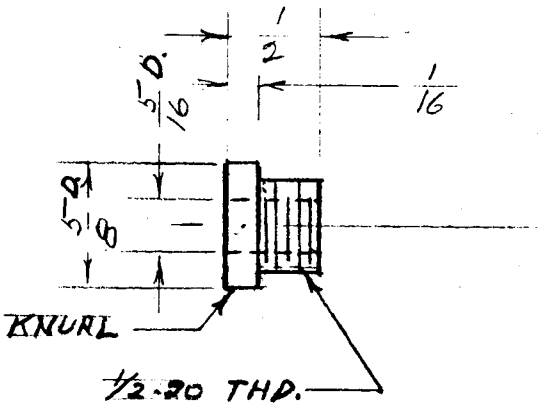

Pt. (15) RETAINER NUT
MAT. ?
PCS. REQ'D - 16

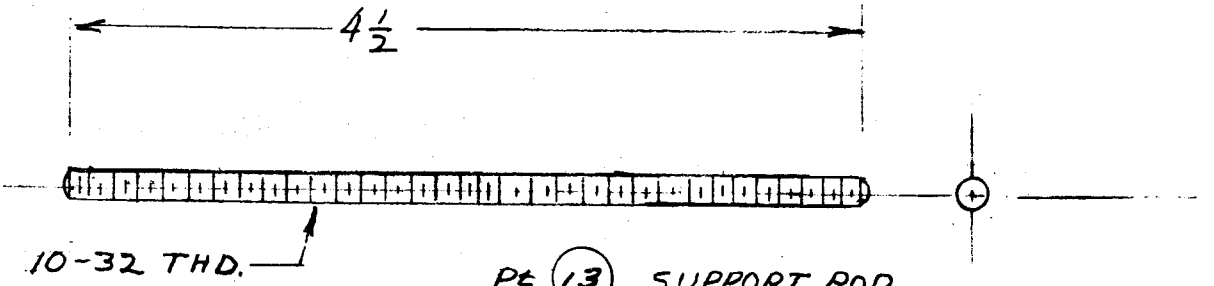

Pt. (13) SUPPORT ROD
MAT. 302 ST. ST
PCS. REQ'D 32

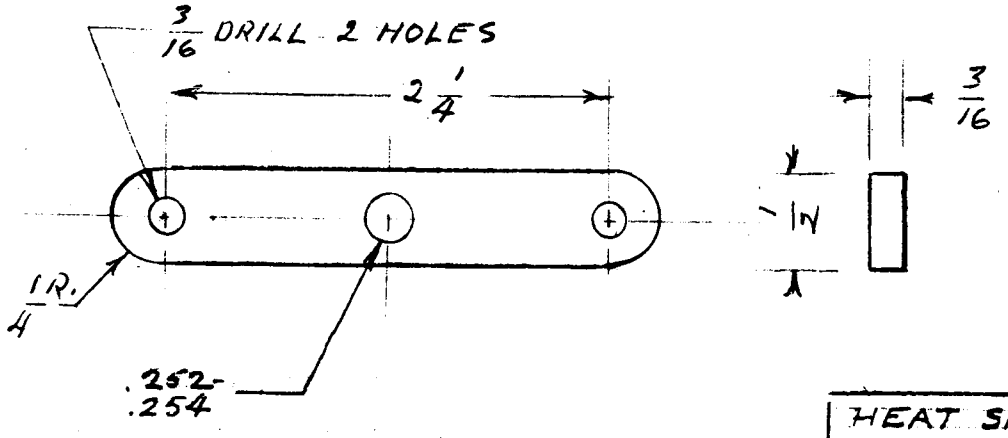

Pt # (12) ROD BEARING
MAT. : 302 ST. ST.
PCS. REQ'D : 32

HEAT SINK PARTS
PROJECT C-567
TYCO LABORATORIES INC.
WALTHAM, MASS

Thermoelectric Material Life Test Device Parts List
Project C-567

Pt. #	Part Description	Pieces Required
1.	Base Plate - 303 S.S.	1
2.	Heater Ring - 302 S.S.	1
3.	Heater Ring Clamps - 302 S.S.	1
4.	Water Manifold - Brass	1
5.	Heat Sink - Copper	16
6.	Bell Jar - Corning 95500	1
7.	Pressure Rod - 303 S.S.	16
8.	Top Thermal Insulator - Fired Lava	16
9.	Inside Thermal Insulator - Fired Lava	1
10.	Outside Thermal Insulator - Fired Lava	1
11.	Outside Thermal Insulator - Fired Lava	1
12.	Rod Bearing - 303 S.S.	32
13.	Support Rod - 303 S.S.	32
14.	Thermocouple Spring Nut - 302 S.S.	16
15.	Retainer Nut - Brass	16
16.	Heater Element - Chromalox Incoloy Sheet Type T1-600W	2
17.	Ferrule Nut - Brass	64
18.	Inlet Tubing - Nylon	16
19.	Outlet Tubing - Nylon	16
20.	Heater Assem. Base Plate - C.R.S.	1
21.	Heater Assem. Support Rod - 302 S.S.	4
22.	Device Support Rod - 302 S.S.	4
23.	Bell Jar Gasket - Butyl Rubber	1
24.	Bell Jar Clamping Ring - Brass	1
25.	Clamp Ring Bolt - 303 S.S.	6
26.	Electrical Feed Thru- Conax PL 12A4	1
	TG 20A16T	5
27.	Heater Clamp Ring Bolt - 302 S.S.	8
28.	Upper Thermocouple Insulator - Alumina	16
29.	Lower Thermocouple Insulator - Alumina	16
30.	Upper Thermocouple Spring Plate - Teflon	16
31.	Lower Thermocouple Spring Plate - Fired Lava	16
32.	Lower Thermocouple Spring Plate - 302 S.S.	16
33.	Lower Thermocouple Spring Bolt - 302 S.S.	16
34.	Heat Sink Retainer Spring - Copper Berylium	16
35.	Heat Sink Loading Spring - Spring Steel	16
36.	Upper Thermocouple Spring - Spring Steel	16
37.	Bearing Plate Nut - 303 S.S.	64
38.	Inlet Elbow - Copper	1
39.	Outlet Elbow - Copper	1
40.	Heater Assem. Casing - 303 S.S.	1
41.	Support Rod Stud - 303 S.S.	4
42.	Test Sample Retainer Ring - 302 S.S.	16
43.	Top Insulator Retainer Nut - 322 S.S.	16